HAL open science

Hölder Exponents and Fractal Analysis on Metric Spaces using Morphological Operators

Jesus Angulo

▶ To cite this version:

Jesus Angulo. Hölder Exponents and Fractal Analysis on Metric Spaces using Morphological Operators. 2022. hal-03108997v2

HAL Id: hal-03108997
https://hal.science/hal-03108997v2

Preprint submitted on 24 Aug 2022

HAL is a multi-disciplinary open access archive for the deposit and dissemination of scientific research documents, whether they are published or not. The documents may come from teaching and research institutions in France or abroad, or from public or private research centers.

L'archive ouverte pluridisciplinaire **HAL**, est destinée au dépôt et à la diffusion de documents scientifiques de niveau recherche, publiés ou non, émanant des établissements d'enseignement et de recherche français ou étrangers, des laboratoires publics ou privés.

Hölder Exponents and Fractal Analysis on Metric Spaces using Morphological Operators

Jesús Angulo

MINES ParisTech, PSL-Research University,
CMM-Centre de Morphologie Mathématique; France

jesus.angulo@mines-paristech.fr

July 2020 *

Abstract

In this work, we are interested in the study of the local and global regularity of a class of functions which are relevant in fractal analysis, the so-called Hölder continuous functions. Indeed, fractal dimension and Hölder exponent of functions are related in many cases. Estimates of the dimension or the exponent of this kind of functions are classicaly based either on wavelet theory or on multiscale morphological operators. In this paper, Hölder function characterization is revisited from the mathematical morphology viewpoint, including the connection with some contributions from the field of max-plus mathematics. We show in particular that morphological operators on metric spaces are naturally formulated in the case of equicontinuous functions, including Hölder functions. We focus on the case of morphological semigroups on length spaces since they provide the natural extension of multiscale morphological operators on the Euclidean space. We prove how these semigroups can be used to characterize the exponent of Hölder functions on length spaces.

Contents

1 Introduction **2**

2 Preliminaries **4**

2.1 Hölder continuous functions 4

2.2 Wavelet transform and Hölder exponent estimation 5

2.3 Morphological gradient and morphological total variation 7

2.4 Gondran's $(\min, +)$-wavelets 9

*Version 2. January 2021

3 Lattice of equicontinuous functions **12**
3.1 Equicontinuous functions 12
3.2 Complete lattice structure 13
3.3 Metric dilation and erosion on $\bar{\mathcal{L}}_m$ 15
3.4 Equicontinuous modulus estimation using morphological operators 20

4 Morphological semigroups on length spaces **20**

5 Fractal dimension, fractal functions and mathematical morphology **23**
5.1 From fractal dimension to fractal functions 23
5.2 Classical fractal analysis using morphological operators on Euclidean space . 28
5.3 Hölder exponent estimation and fractal analysis in max-plus mathematics . . 33

6 Morphological multiscale analysis on the lattice of Hölder functions on metric spaces **37**
6.1 Dilation and erosion semigroups on the lattice of Hölder functions on length spaces 38
6.2 Hölder exponent estimates on length spaces 43
6.3 Experimental validation 45

7 Conclusions and perspectives **53**

1 Introduction

In mathematics, fractal sets and fractal functions can be considered under two different viewpoints, either from their non-integer dimension or from their self-similarity behaviour [25, 38]. Fractals can be used as random models for sets and functions. In comparison to many other stochastic models, where the main intrinsic invariance is associated to the translation (i.e., stationarity), fractals are invariant by homothetic deformations (i.e., statistical phenomenon is equal to itself at all the scales). An important remark also is the fact that the self-similarity is a global property, whereas the measure of the dimension is on the contrary a local one. Here we basically adopt the description of fractal sets and functions by their local regularity, which is related to their fractal dimension. We note, by the way, there is not a unique definition of the fractal dimension [25]. More specifically, we are interested in the study of the global and local regularity of a class of functions which are relevant in fractal analysis, the so-called Hölder continuous functions. Indeed, fractal dimension and Hölder exponent of functions are related in many cases. Estimates of the dimension and the exponent of this kind of functions are classicaly based either on wavelet theory [27] or on multiscale morphological operators.

Mathematical morphology is a nonlinear image processing methodology based on two basic operators, dilation and erosion, which correspond respectively to the convolution in the

$(\max, +)$ algebra and its dual. More precisely, in Euclidean (translation invariant) mathematical morphology the pair of adjoint and dual operators, dilation (sup-convolution) $(f \oplus b)(x)$ and erosion (inf-convolution) $(f \ominus b)(x)$ of an image $f : E \subset \mathbb{R}^n \to \overline{\mathbb{R}} = \mathbb{R} \cup \{-\infty, +\infty\}$, $f \in \mathcal{F}(E, \overline{\mathbb{R}})$, are given by [39, 40]:

$$\begin{cases} \delta_b(f)(x) = (f \oplus b)(x) = \sup_{y \in E} \{f(y) + b(x-y)\}, \\ \\ \varepsilon_b(f)(x) = (f \ominus b)(x) = \inf_{y \in E} \{f(y) - b(y-x)\}, \end{cases} \tag{1}$$

where $b : \mathbb{R}^n \to \overline{\mathbb{R}}$ is the structuring function which determines the effect of the operator. The structuring function plays a similar role to the kernel in classical convolution filtering. The structuring function is typically a parametric family $b_\lambda(x)$, where $\lambda > 0$ is the scale parameter. In particular, the canonic structuring function is the parabolic shape (i.e., square of the Euclidean distance):

$$b_\lambda(x) = q_\lambda(x) = -\frac{\|x\|^2}{2\lambda}.$$

such that the corresponding dilation and erosion are equivalent to the Lax-Oleinik operators or viscosity solution of the standard Hamilton-Jacobi PDE: $u_t(t,x) \mp \|u_x(t,x)\|^2 = 0$, $(t,x) \in (0, +\infty) \times E$; $u(0,x) = f(x)$, $x \in E$. Theory of morphological filtering is based on opening and closing operators, obtained respectively by product composition of erosion-dilation and dilation-erosion. Opening (resp. closing) is increasing, idempotent and anti-extensive (resp. extensive). Evolved filters are obtained by composition of openings and closings [39, 40]. Morphological operators are classically defined for images supported on Euclidean spaces. However, different imaging modalities produce nowadays images on smooth surfaces represented by meshes. Other datasets which do not fit the Euclidean framework are the case of functions on graphs or on point clouds, which are more properly modelled as metric space. Mathematical morphology operators and semigroups are naturally extended to real-valued functions whose support space is a Riemannian manifold [1] or a length space [3].

In this study, Hölder function characterization is revisited from the mathematical morphology viewpoint, including the connection with some contributions from the field of max-plus mathematics [13, 14]. Relationship between morphology and fractals is rather natural since Minkowski dimension of a set is based on a measure from a scaled Minkowski sum of the set with a ball. The first contributions dealing with that practical method to connect a morphological measure of local oscillation and fractal dimension focussed on the 1D case [46, 47] and were then extended to the 2D case (images) [36, 45, 28, 29]. The case of the application of morphological fractal analysis to speech recognition, motivated by the physics of speech aerodynamics and connected to turbulence flow, is also remarkable [31]. For other applications on physics and engineering, see for instance [38].

Readers interesting on the application viewpoint of fractals models in image and signal processing are referred to [22], where a systematic review of fractal (and multifractal) analysis applications like pattern recognition, texture analysis and segmentation in the field of

medical signal/image analysis is considered. More recently, estimation of Hurst index characterizing fractional Brownian motions on surfaces [18] has been considered using spectral representation of surfaces built upon their Laplace–Beltrami operator [35], with applications on brain surfaces from MRI.

Paper organization. The rest of this document is organized as follows.

- Background notions are discussed in Section 2.
- Section 3 studies the properties of morphological operators on metric spaces for general equicontinuous functions.
- The specific case of morphological semigroups of length spaces is reviewed in Section 4.
- The goal of Section 5 is to review the application of morphological operators in Euclidean spaces for the estimation of fractal dimension and Hölder exponent.
- In Section 6, we introduce the generalization to the metric space case, where morphological multiscale operators are used to provide Hölder exponent estimation on that setting.
- Conclusions and perspectives in Section 7 close the paper.

2 Preliminaries

The goal of this section of to review some background material which is required for the sequel.

2.1 Hölder continuous functions

A function $f : \mathbb{R}^n \to \mathbb{R}$ is an α-Hölder continuous function, or Hölderian function, for which it exists the exponent α, $0 < \alpha \leq 1$, and a constant K, when the following condition is satisfied

$$|f(x) - f(y)| \leq K\|x - y\|^{\alpha}, \quad \forall x, y \in \mathbb{R}^n, \ K > 0. \tag{2}$$

Obviously if $\alpha = 1$, then the function satisfies a Lipschitz condition. So, if α is known, we do have

$$\mathrm{Lip}_{\alpha}(f) = \sup \left\{ \frac{|f(x) - f(y)|}{\|x - y\|^{\alpha}}; \ x, y \in \mathbb{R}^n, \ x \neq y \right\}.$$

The regularity Hölder condition (2) is a sufficient but not necessary condition for a function to be continuous. In the case of fractal functions, the exponent α is related to its fractal dimension [25].

The condition (2) can be also formulated for functions between any two metric spaces. Namely, let (X, d) be a metric space and consider the real-valued function $f : X \to \mathbb{R}$. Then,

we say that f is α-Hölder in X with exponent $0 < \alpha \leq 1$ if there exists a constant $K > 0$ such that

$$|f(x) - f(y)| \leq K d(x,y)^{\alpha}, \quad \forall x, y \in X. \tag{3}$$

We note that Hölder continuity condition here is a global one. It requires that the inequality holds for all pair of points. However, it is often good enough to have the condition locally, i.e., for every compact set $\mathcal{K} \subset X$, there is a constant $K_{\mathcal{K}}$ for which the condition holds with that constant.

2.2 Wavelet transform and Hölder exponent estimation

Let us review the main results on the interest of wavelet transform to quantitatively deal with Hölder regularity. We follow [27](Chapter 6).

The α-Hölder regularity of f over $\mathbb{R}$ is related to the asymptotic decay of its Fourier transform. More precisely, a function f is bounded and α-Hölder over $\mathbb{R}$ if [27]

$$\int_{-\infty}^{\infty} \left|\hat{f}(\omega)\right| (1 + |\omega|^{\alpha})\, d\omega < +\infty$$

where $\hat{f}(\omega) = \int_{-\infty}^{\infty} f(x) \exp(-iwx) dx$ is the Fourier transform of f. This expression provides a measure of the minimum global regularity; however, it is not possible to analyze the regularity of f at a particular point x from the decay of $\left|\hat{f}(\omega)\right|$ at high frequencies ω.

To measure the local regularity of a signal, wavelet transform can be used, where the requirement for the wavelet is to have vanishing moments, which are related to the exhibiting oscillations. If the wavelet has n vanishing moments then the wavelet transform can be interpreted as a multiscale differential operator of order n [27]. A wavelet is a function ψ with a zero average, i.e., $\int_{-\infty}^{\infty} \psi(x) dx = 0$, and n vanishing moments, i.e., $\int_{-\infty}^{\infty} x^m \psi(x) dx = 0$, $1 \leq m \leq n$. The wavelet is "dilated" at scale $s > 0$,

$$\psi_s(x) = \frac{1}{\sqrt{s}} \psi\left(\frac{-x}{s}\right),$$

and translated at point y

$$\psi_{x,s}(y) = \frac{1}{\sqrt{s}} \psi\left(\frac{y-x}{s}\right).$$

Then, the wavelet transform of signal f is defined as

$$Wf(x,s) = f \star \psi_s(x) = \langle f, \psi_{x,s} \rangle = \int_{-\infty}^{\infty} f(z) \frac{1}{\sqrt{s}} \psi\left(\frac{z-x}{s}\right) dz, \tag{4}$$

where the s-scaled wavelet is

$$\bar{\psi}_s(x) = \frac{1}{\sqrt{s}} \psi\left(\frac{-x}{s}\right).$$

Let us also recall the (Calderón, Grossmann and Morlet) reconstruction formula [27]: any $f \in L^2(\mathbb{R})$ satisfies

$$f(x) = C_\psi^{-1} \int_0^\infty \int_{-\infty}^\infty Wf(u,s) \frac{1}{\sqrt{s}} \psi\left(\frac{t-u}{s}\right) du \frac{ds}{s^2}, \text{ with } C_\psi = \int_0^\infty \frac{|\psi(w)|^2}{w} dw < +\infty. \quad (5)$$

The decay of the wavelet transform amplitude across scales is related to the pointwise reglarity of the signal. Measuring the decay is equivalent to zooming into signal structures with a scale that goes to zero. More precisely, we have, on the one hand, the following result of the global Hölder regularity of f on an interval.

Theorem 1 (Mallat, 2008 [27]) *Let us suppose that the wavelet ψ has n vanishing moments. If $f \in L^2(\mathbb{R})$ is α-Hölder with $\alpha \leq n$ over $[a,b]$, then there exists $A > 0$ such that $\forall \alpha \in \mathbb{R}_+$*

$$|Wf(x,s)| \leq As^{\alpha+1/2}, \ \forall x \in \mathbb{R}. \quad (6)$$

Conversely, suppose that f is bounded and that $Wf(x,s)$ satisfies (6) for an $\alpha < n$ that is not an integer. Then f is α-Hölder on $[a+\epsilon, b-\epsilon]$, for any $\epsilon > 0$.

When the scale s decreases, $Wf(x,s)$ measures fine scale variations in the local neighborhood of x. Indeed, the inequality (6) is a condition on the asymptotic decay of $|Wf(x,s)|$ when s goes to zero. At large scales it does not introduce any constraint since the Cauchy–Schwarz inequality guarantees that the wavelet transform is bounded: $|Wf(x,s)| = |\langle f, \psi_{x,s}\rangle| \leq \|f\|\|\psi\|$.

On the other hand, we have the following result which gives a necessary condition and a sufficient condition on the wavelet transform for estimating the Hölder regularity of f at a given point y.

Theorem 2 (Jaffard and Meyer, 1996 [17]) *If $f \in L^2(\mathbb{R})$ is α-Hölder with $\alpha \leq n$ at y, then there exists A such that $\forall \alpha \in \mathbb{R}_+$*

$$|Wf(x,s)| \leq As^{\alpha+1/2}\left(1 + \left|\frac{x-y}{s}\right|^\alpha\right), \ \forall x \in \mathbb{R}. \quad (7)$$

Conversely, if $\alpha < n$ is not an integer and there exist A and $\alpha' < \alpha$ such that $\forall \alpha \in \mathbb{R}^+$

$$|Wf(x,s)| \leq As^{\alpha+1/2}\left(1 + \left|\frac{x-y}{s}\right|^{\alpha'}\right), \ \forall x \in \mathbb{R}. \quad (8)$$

then f is α-Hölder at y.

We can now consider the particular case of wavelet which is defined by the derivative of the Gaussian filter. This framework was considered for the case of singularity characterisation, for instance in multiscale edge detection [26].

To deal with border of gray level images which are typically infinitely continuously differentiable, the edge transition is modeled as as a diffusion with a Gaussian kernel that has a variance that is measured from the decay of wavelet modulus maxima. Thus, in the neighborhood of a sharp transition at point x,we suppose that

$$f(x) = f_0 \star g_\sigma(x),$$

where g_σ is a Gaussian kernel of variance σ^2:

$$g_\sigma(x) = \frac{1}{\sigma\sqrt{2\pi}} \exp\left(\frac{-x^2}{2\sigma^2}\right).$$

If f_0 has a α-Hölder singularity at x that is isolated and nonoscillating, it is uniformly α-Hölder in the neighborhood of x. For wavelets that are derivatives of Gaussians, the following theorem relates the decay of the wavelet transform to σ and α.

Theorem 3 (Mallat and Zhong, 1992 [26]) *Let $\psi(x) = (-1)^n\theta^n(x) = (-1)^n \frac{d^n}{dx^n}\theta(x))$ with $\theta(x) = \lambda \exp\left(-x^2/(2\beta^2)\right)$. If $f = f_0 \star g_\sigma$ and f_0 is uniformly α-Hölder on $[x-h, x+h]$, then there exists A such that*

$$|Wf(x,s)| \leq As^{\alpha+1/2}\left(1 + \frac{\sigma^2}{\beta^2 s^2}\right)^{-(n-\alpha)/2}, \ \forall (x,s) \in [x-h, x+h] \times \mathbb{R}^+. \tag{9}$$

This theorem explains the interaction between the Gaussian averaging and the wavelet tranform: at large scales $s \gg \sigma/\beta$, the Gaussian filtering is not afected by the wavelet transform that decays like $s^{\alpha+1/2}$. For $s \leq \sigma/\beta$, the variation of f at x is not sharp relative to s because of the Gaussian averaging. At these fine scales, the wavelet transform decays like $s^{n+1/2}$ because f is infinitely continuously differentiable.

The variance β^2 depends on the choice of wavelet and is known in advance. Using this kind of result, the parameters A, α, and σ are numerically estimated from a regression in log–log scale to approximate

$$\log|Wf(x,s)| \approx \log A + \left(\alpha + \frac{1}{2}\right)\log s - \left(\frac{n-\alpha}{2}\right)\log\left(1 + \frac{\sigma^2}{\beta^2 s^2}\right). \tag{10}$$

In summary, the wavelet transform amplitude across scales is related to the local signal regularity and Hölder exponents. In this work, we show similar relationships obtained from morphological operators.

2.3 Morphological gradient and morphological total variation

By simplicity, let us consider the two dimensional case, i.e., $f : \mathbb{R}^2 \to \mathbb{R}$. The directional derivative of f in direction ω is given by

$$\begin{aligned} \nabla_\omega f(x) &= \frac{df}{dh_\omega} = \frac{\partial f}{\partial x_1}\cos\omega + \frac{\partial f}{\partial x_2}\sin\omega = \langle \nabla f(x), u_\omega \rangle \\ &= \rho\cos(\theta - \omega), \end{aligned}$$

where ρ and θ are respectively the modulus and the direction of ∇f at point x. The connection with morphological operators is classical [39]. Let us introduce the elementary dilation and erosion in direction ω:

$$\begin{aligned} \delta_\omega f(x) &= \sup\{f(x), f(x+dh_\omega)\}, \\ \varepsilon_\omega f(x) &= \inf\{f(x), f(x+dh_\omega)\}. \end{aligned}$$

Then

$$\frac{\delta_\omega f(x) - \varepsilon_\omega f(x)}{dh_\omega} = \left|\frac{df}{dh_\omega}\right| = \rho\,|\cos(\theta-\omega)|,$$

and by averaging over ω:

$$|\nabla f(x)| = \frac{1}{4}\int_0^{2\pi} \frac{\delta_\omega f(x) - \varepsilon_\omega f(x)}{dh_\omega} d\omega.$$

From this expression, the morphological gradient (also known as Beucher's gradient [39](pp. 440-441)) is given by

$$\beta(f)(x) = \lim_{\lambda\to 0} \frac{(f\oplus\lambda B)(x) - (f\ominus\lambda B)(x)}{2\lambda},$$

where B is a closed unit disk in $\mathbb{R}^n$, and which equals $|\nabla f(x)|$ almost everywhere. In the discrete case of unit ball B, one may use the classical expression $\beta_B(f)(x) = (f\oplus B)(x) - (f\ominus B)(x)$, which can be generalized to the notion of *morphological gradient* by structuring function $b(x)$ as

$$\beta_b(f)(x) = (f\oplus b)(x) - (f\ominus b)(x). \tag{11}$$

For more details on morphological gradients, the reader is referred to [37].

The norm of the gradient of the function is used to define the notion of total variation. Namely, let Ω be an open subset of $\mathbb{R}^n$ and f a function belonging to $L^1(\Omega)$, its total variation is

$$TV(f) = \int_\Omega |\nabla f(x)|\, dx.$$

For a real-valued continuous function f, defined on an interval $[a,b]\subset\mathbb{R}$, its total variation is a measure of the one dimensional arclength of the curve $x\mapsto f(x)$. Analytically, the corresponding expression is given by

$$TV(f) = \sup_{\mathcal{P}} \sum_{i=0}^{P-1} |f(x_{i+1}) - f(x_i)|,$$

where the supremum runs over the set of all partitions $\mathcal{P} = \{\ \pi = \{x_0,\cdots,x_P\} : \pi$ is a partition such that $x_0 = a$ and $x_p = b\ \}$.

It seems therefore natural to introduce the notion of *morphological total variation* for any function $f : \mathbb{R}^2 \to \mathbb{R}$ with respect to a structuring fucntion b as

$$MTV_b(f) = \int_\Omega \beta_b(f)(x)dx = \int_\Omega \left[(f \oplus b)(x) - (f \ominus b)(x) \right] dx. \tag{12}$$

This quantity will appear below for estimating the fractal dimension.

2.4 Gondran's $(\min, +)$-wavelets

$(\min, +)$-analysis and the corresponding wavelets have been mainly developed by Gondran [11, 12], see also the excellent book [32]. It is intimely related to mathematical morphology and because two basic references to our work [13, 14] used $(\min, +)$-wavelets, we briefly revisit the main elements.

First, let us introduce the notion $(\min, +)$-scalar product which consists in replacing in the scalar product definition of two real-valued functions $f, g : X \to \mathbb{R}$, the real number field $(\mathbb{R}, +, \times)$ by the $(\min, +)$ dioid $(\mathbb{R} \cup +\infty, \min, +)$. The classical scalar product $\langle f, g \rangle = \int_X f(x)g(x)dx$ becomes then the $(\min, +)$-scalar product [11]:

$$\langle f, g \rangle_{(\min,+)} = \inf_{x \in X} \{ f(x) + g(x) \}.$$

As a scalar product within the $(\min, +)$ dioid, it satisfies [13]:

- Symmetry:

$$\langle f, g \rangle_{(\min,+)} = \langle g, f \rangle_{(\min,+)}.$$

- Positive definite with respect to $+\infty$ (neutral element in $(\min, +)$ dioid):

$$\langle f, g \rangle_{(\min,+)} \leq +\infty.$$

  Proof. Since $+\infty$ is the neutral element of the min operator, if $\langle f, g \rangle_{(\min,+)}$, then $f(x) = +\infty$ for all $x \in X$. Furthermore, in the dioid $(\min, +)$ dioid the notion of "bigger or equal to" corresponds to $\leq$ in the field of real numbers. ■

- Linearity with respect the addition of a constant and the minimum of two functions:

$$\langle f, \lambda + g \rangle_{(\min,+)} = \lambda + \langle f, g \rangle_{(\min,+)}, \quad \lambda \in \mathbb{R},$$

$$\langle f, \min(g_1, g_2) \rangle_{(\min,+)} = \min \left(\langle f, g_1 \rangle_{(\min,+)}, \langle f, g_2 \rangle_{(\min,+)} \right).$$

  Proof. The first part is obvious since

$$\inf_{x \in X} \{ f(x) + \lambda + g(x) \} \quad = \quad \lambda + \inf_{x \in X} \{ f(x) + g(x) \}.$$

For the distributibity with respect to the minimum of two functions, the equality will be proven using two inequalities. First, two obvious relations:

$$\langle f, g_1\rangle_{(\min,+)} \leq f(x) + g_1(x), \text{ and } \langle f, g_2\rangle_{(\min,+)} \leq f(x) + g_2(x), \ x \in X,$$

which gives

$$\min\left(\langle f, g_1\rangle_{(\min,+)}, \langle f, g_2\rangle_{(\min,+)}\right) \leq \min\left(f(x) + g_1(x), f(x) + g_2(x),\right), \ x \in X,$$

Using the fact that

$$\min\left\{f(x) + g_1(x), f(x) + g_2(x)\right\} = f(x) + \min\left\{g_1(x), g_2(x)\right\},$$

one there has

$$\min\left(\langle f, g_1\rangle_{(\min,+)}, \langle f, g_2\rangle_{(\min,+)}\right) \leq f(x) + \min\left(g_1(x), g_2(x)\right), \ x \in X,$$

which provides the first inequality

$$\min\left(\langle f, g_1\rangle_{(\min,+)}, \langle f, g_2\rangle_{(\min,+)}\right) \leq \langle f, \min(g_1, g_2)\rangle_{(\min,+)}. \tag{13}$$

For the second step, we start from

$$\langle f, \min(g_1, g_2)\rangle_{(\min,+)} \leq f(x) + \min\left(g_1(x), g_2(x)\right) \leq f(x) + g_1(x), \ x \in X,$$

which becomes

$$\langle f, \min(g_1, g_2)\rangle_{(\min,+)} \leq \langle f, g_1\rangle_{(\min,+)}.$$

A similar inequality is obtained for g_2, which combined, will provide

$$\langle f, \min(g_1, g_2)\rangle_{(\min,+)} \leq \min\left\{\langle f, g_1\rangle_{(\min,+)}, \langle f, g_2\rangle_{(\min,+)}\right\}. \tag{14}$$

From (13) and (14), we obtain the equality of the distributivity. ■

In $(\min, +)$-analysis, for any lower semi-continuous (l.s.c.) function $f : \mathbb{R}^n \to \overline{\mathbb{R}}$, the following (lower hull) transform of f is introduced [11, 32]:

$$T_f^-(a, b) = \inf_{x\in\mathbb{R}^n}\left\{f(x) + h\left(\frac{x-b}{a}\right)\right\}, \ b \in \mathbb{R}^n, \ a \in \mathbb{R}_+, \tag{15}$$

where h is a basis analysing function, which is an upper semi-continuous (u.s.c.) and inf-compact and it should satisfy $h(0) = 0$. Typical functions are

$$\begin{aligned} h_\alpha(x) &= \frac{\|x\|^\alpha}{\alpha}, \ \alpha > 1, \\ h_\infty(x) &= \{0, \text{ if } \|x\| \leq 1, \ +\infty \text{ else}\}. \end{aligned}$$

Using (15), the function can be resconstructed using a similar approach than the reconstruction formula from a wavelet basis (5). Hence, any lower bounded and l.s.c f satisfies [13]:

$$f(x) = \sup_{a\in\mathbb{R}_+} \sup_{b\in\mathbb{R}^n} \left\{ T_f^-(a,b) - h\left(\frac{x-b}{a}\right)\right\}, \tag{16}$$

which using $(\min,+)$ calculus, i.e., $x = b \implies h(0) = 0$, we get

$$f(x) = \sup_{a\in\mathbb{R}_+} T_f^-(a,x).$$

Similarly, the upper hulls are defined as

$$T_f^+(a,b) = \sup_{x\in\mathbb{R}^n} \left\{ f(x) - h\left(\frac{x-b}{a}\right)\right\}, \;\; b\in\mathbb{R}^n, \;\; a\in\mathbb{R}_+, \tag{17}$$

with the corresponding reconstrucction formula:

$$\begin{aligned} f(x) &= \inf_{a\in\mathbb{R}_+} \inf_{b\in\mathbb{R}^n} \left\{ T_f^+(a,b) + h\left(\frac{x-b}{a}\right)\right\}, \\ &= \inf_{a\in\mathbb{R}_+} T_f^+(a,x). \end{aligned} \tag{18}$$

The $(\min,+)$ analysis is based on the simultaneous analysis of lower hulls $T_f^-(a,b)$ and upper hulls $T_f^+(a,b)$: the $(\min,+)$ *wavelet* is defined as the pair $\left(T_f^-(a,b), T_f^+(a,b)\right)$. Then, the a-oscillation of f is defined as

$$\Delta T_f(a,b) = T_f^+(a,b) - T_f^-(a,b). \tag{19}$$

The case of h_∞ in $1D$ gives

$$\Delta T_f(a,b) = \sup_{|b-y|\leq a} \{f(y)\} - \inf_{|b-z|\leq a} \{f(z)\} = \sup_{x,z\in[b-a,b+a]} \{|f(y)-f(z)|\},$$

which is just the so-called Tricot a-oscillation [47].

Using the classical formulation of morphological operators (1) and by identification with (15) and (17), we remark that $T_f^-(a,b)$ is an erosion and $T_f^+(a,b)$ a dilation with a multiscale p-power structuring function:

$$(f \oplus b_{P,\lambda})(x) = T_f^+(\lambda,x); \;\; (f \ominus b_{P,\lambda})(x) = T_f^-(\lambda,x).$$

where

$$\begin{aligned} b_{P,\lambda}(x) &= -h_P\left(\frac{x}{\lambda}\right) = -\frac{\|x\|^P}{P\lambda^P}, \;\; P>1, \\ b_{\infty,\lambda}(x) &= -h_\infty\left(\frac{x}{\lambda}\right) = \{0, \text{ if } \|x\|\leq\lambda, \;\; -\infty \text{ else}\}. \end{aligned}$$

Therefore, the a-oscillation $\Delta T_f(a,b)$ corresponds to the morphological gradient: $\Delta T_f(a,b) = \beta_{b_{P,\lambda}}(f)(x)$.

In the rest of the paper, we use our notation on morphological operators when we refer to the results from [13, 14].

3 Lattice of equicontinuous functions

Morphological operators are defined in the general framework of complete lattices [40, 16]. For the case of numerical functions, we adopt here the model developped by Serra [41, 42, 43] for equicontinuous functions. Indeed, the classes of equicontinuous functions offer a remarkably consistent theoretical framework to morphological operators. Besides the properties of continuity, equicontinuous functions are closed under supremum and infimum as well as under addition and subtraction. It provides also a more symmetrical framework for scalar dilation and erosion than the semi-continuous functions, which is the alternative approach to deal with numerical functions in scalar morphology [39, 40, 16]. The case of the complete lattice for Lipschitz functions was independiently studied in [34].

The motivation for this study is rather natural since Hölder continuous functions are a particular case of equicontinous functions.

3.1 Equicontinuous functions

Let (X, d) be a metric space. We assume that d is the Euclidean distance when $X = \mathbb{R}^n$ or the geodesic distance $d_{\mathcal{M}}$ when X is a Riemannian manifold $\mathcal{M}$. Let us consider the family of functions $f : X \to \mathbb{R}$, $f \in \mathcal{F}(X, \mathbb{R})$.

Uniform continuity. A function $f \in \mathcal{F}(X, \mathbb{R})$ is uniformly continuous if $\forall \epsilon > 0,\ \exists \delta > 0,$ $\forall x, y \in D :\ d(x, y) < \delta \ \Rightarrow\ |f(x) - f(y)| < \epsilon$, whereas f is continuous if $\forall x \in D,\ \forall \epsilon > 0,$ $\exists \delta > 0\ \forall y \in D :\ d(x, y) < \delta \ \Rightarrow\ |f(x) - f(y)| < \epsilon$. The difference between uniform continuity and ordinary continuity at every point, is that in uniform continuity the value of δ depends only on ϵ and not on the point in the domain. Continuous functions can fail to be uniformly continuous if they are unbounded on a finite domain or if their slopes become unbounded on an infinite domain.

Modulus of continuity. Let $m : \mathbb{R}_+ \to \mathbb{R}_+$ be an increasing map, continuous and such that $m(0) = 0$ and sub-additive $m(h + k) \leq m(h) + m(k)$. Then, the function $f \in (X, \mathbb{R})$ is said to admit m as modulus of continuity when one has

$$|f(x) - f(y)| \leq m\left(d(x, y)\right), \quad \forall x, y \in \mathbb{R}^n. \tag{20}$$

Equicontinuous functions. A function $f \in \mathcal{F}(X, \mathbb{R})$ is equicontinuous with respect to modulus m, or more briefly, is a m-continuous function when, given m, if (20) holds. Similarly the family of all functions $f \in \mathcal{F}(X, \mathbb{R})$ which satisfy inequality (20) is called m-continuous and it is denoted by $f \in \mathcal{L}_m$.

It is obvious that the following inclusion order exists between equicontinuous functions

$$m_1 \leq m_2 \implies \mathcal{L}_{m_1} \subseteq \mathcal{L}_{m_2} \tag{21}$$

The members of the m-continuous classes are uniformly continuous functions. Namely, an equicontinuous collection of functions have a single $\delta = \delta(\epsilon)$ can be chosen for any arbitrary ϵ so as to make all $f \in \mathcal{L}_m$ uniformly continuous simultaneously, independent of f. In general, the role of $m(h)$ is to fix some explicit functional dependence of ϵ on δ in the (ϵ, δ) definition of uniform continuity [8]. Typical examples are

- Lipschitz functions: $m(h) = Kh$;
- α-Hölder functions $m(h) = Kh^{\alpha}$.

The following result is natural and well known.

Proposition 4 *For a given modulus of continuity m, the space of equicontinuous functions $\mathcal{L}_m$ is closed under inversion and addition of a constant. That is, for $f \in \mathcal{L}_m$ and $c \in \mathbb{R}$, we have $-f \in \mathcal{L}_m$ and $c + f \in \mathcal{L}_m$.*

In addition, $\mathcal{L}_m$ is convex, which means that for $f, g \in \mathcal{L}_m$ for $k \in [0, 1]$, we have $k\, f + (1 - k)\, g \in \mathcal{L}_m$.

It is easy to see that the constant functions belong to $\mathcal{L}_m$.

As a consequence of this proposition, concerning linear transformations of $f \in \mathcal{L}_m$, one has that the convolution of f with a finite kernel k, such that $\nu = \int_X |k(x)|dx$, has a modulus of continuity equal to $m' = \nu m$, i.e., $(f \star k) \in \mathcal{L}_{\nu m}$. The proof is straightforward:

$$\begin{aligned} |(f \star k)(x) - (f \star k)(y)| &= \left| \int_X (f(x-z) - f(y-z))k(z)dz \right| \\ &\leq \left| \int_X (f(x) - f(y))k(z)dz \right| \leq m(d(x,y)) \int_X |k(x)|dx = \nu m(d(x,y)). \end{aligned}$$

Therefore, the class $\mathcal{L}_m$ is stable for convolution with $\nu = 1$ and closed when $\nu \leq 1$, as well as for the semi-difference between f and an operator ϕ stable in $\mathcal{L}_m$ of type $1/2(f - \phi(f))$.

3.2 Complete lattice structure

A partially ordered set $(\mathcal{L}, \leq)$ is a complete lattice if every subset of $\mathcal{L}$ has both a greatest lower bound (the infimum $\bigwedge$, also called the meet) and a least upper bound (the supremum $\bigvee$, also called the join) in $(\mathcal{L}, \leq)$. Given a lattice $\mathcal{L}$, a subset $\mathcal{L}' \subset$ is a sublattice when $\mathcal{L}'$ under the $\bigwedge$ and the $\bigvee$ of $\mathcal{L}$ and admits the same two extrema as $\mathcal{L}$. All mappings defined on $\mathcal{L}$, and which involve uniquely supremum and infimum, have a correspondence over $\mathcal{L}'$.

Let us consider the complete lattice of real-valued functions $\mathcal{F}(X, \overline{\mathbb{R}})$, which is naturally endowed with partial order relation $\leq$ defined by setting $f \leq g$ for two functions f and g, if and only if $f(x) \leq g(x)$, $\forall x \in X$. For any two functions $f, g \in \mathcal{F}(X, \overline{\mathbb{R}})$, the join $f \vee g$ and the meet $f \wedge g$ are therefore

$$\begin{aligned} (f \vee g)(x) &= \sup\left[f(x), g(x)\right], \ \forall x \in X, \\ (f \wedge g)(x) &= \inf\left[f(x), g(x)\right], \ \forall x \in X. \end{aligned}$$

For a family $\{f_i,\, i \in I\}$, with $f_i \in \mathcal{F}(X, \overline{\mathbb{R}})$, we define their supremum $\sup_{i\in I} f_i$ and infimum $\inf_{i\in I} f_i$ by setting $\forall x \in X$:

$$\left[\sup_{i\in I} f_i\right](x) = \sup_{i\in I}\left[f_i(x)\right], \quad \left[\inf_{i\in I} f_i\right](x) = \inf_{i\in I}\left[f_i(x)\right].$$

Let ∞_X be the constant function on X having $+\infty$ everywhere. We consider now $\bar{\mathcal{L}}_m = \mathcal{L}_m \cup \{-\infty_X, \infty_X\}$ called the completion of $\mathcal{L}_m$ [4], such that $\bar{\mathcal{L}}_m \subseteq \mathcal{F}(X, \overline{\mathbb{R}})$. Note that $\sup_{i\in\emptyset} f_i = -\infty_X$ and $\inf_{i\in\emptyset} f_i = \infty_X$.

One of the inmediate properties of equicontinuous functions, due to the increaseness of the modulus of continuity, is the fact that they are closed under supremum and infimum, which implies the following result.

Theorem 5 (Serra, 1997 [43]) *For every modulus of continuity m, the class $\bar{\mathcal{L}}_m$ of the m-continuous mappings from X to $\overline{\mathbb{R}}$ is a complete lattice, sublattice of $\mathcal{F}(X, \overline{\mathbb{R}})$.*

Proof. Our proof is generalization of the one provided in [34] for Lipschitz functions. Let $\{f_i,\, i \in I\}$ be a family in $\bar{\mathcal{L}}_m$. Put $f = \sup_{i\in I} f_i$. As I is not empty, $f(x) > -\infty$. Suppose that $f \neq \infty_X$; there is thus some $f(z) \leq \infty$. For $i \in I$ and $x, y \in X$, we have

$$f_i(x) \leq f_i(y) + m\left(d(x,y)\right) \leq f(y) + m\left(d(x,y)\right),$$

and by taking the supremum on all $i \in I$ we get

$$f(x) \leq f(y) + m\left(d(x,y)\right).$$

In particular, for $y = z$ we obtain

$$f(x) \leq f(z) + m\left(d(x,y)\right) \leq \infty;$$

that is, $f(x) \in \mathbb{R}$ for all $x \in X$

$$f(x) - f(y) \leq m\left(d(x,y)\right).$$

Thanks to the symmetry between x and y that is equivalent to

$$|f(x) - f(y)| \leq m\left(d(x,y)\right),$$

and thus f is m-continuous. The case $f = \sup_{i\in I} f_i = \infty_X$ is trivial, since the constant functions are the only elements common to all m-continuous classes

A similar result may also be obtained for $\inf_{i\in I} f_i$, which therefore involves that class $\bar{\mathcal{L}}_m$ is a lattice, closed under the supremum and infimum of $\mathcal{F}(X, \overline{\mathbb{R}})$. ■ We note that the finite products of lattices $\bar{\mathcal{L}}_m$ will be a complete lattice. This generalization is useful for instance in the case of multispectral images.

Given an arbitrary complete lattice, dilation and erosion are two basic operations that preserve the supremum and the infimum. Let us summarize the notion of adjunction [40, 16].

Definition 6 *Let δ and ε be two maps $\mathcal{F}(X,\overline{\mathbb{R}}) \to \mathcal{F}(X,\overline{\mathbb{R}})$. We say that:*

- *δ is a dilation if it commutes with the supremum operation, i.e., for any $\{f_i,\ i \in I\}$, with $f_i \in \mathcal{F}(X,\overline{\mathbb{R}})$, we have*
$$\delta(\sup_{i\in I} f_i) = \sup_{i\in I} \delta(f_i).$$
- *ε is an erosion if it commutes with the infimum operation, i.e., for any $\{f_i, i \in I\}$, with $f_i \in \mathcal{F}(X,\overline{\mathbb{R}})$, we have*
$$\varepsilon(\inf_{i\in I} f_i) = \inf_{i\in I} \varepsilon(f_i).$$
- *(ε,δ) is an adjunction if for every $f,g \in \mathcal{F}(X,\overline{\mathbb{R}})$, we have*
$$\delta(f) \leq g \Longleftrightarrow f \leq \varepsilon(g).$$

The adjunction (ε,δ) provides a bijection between the dilation δ and the erosion ε. Indeed, for every dilation δ (resp. erosion ε) there is a unique erosion ε (resp. dilation δ) such (ε,δ)

Moreover, dilations and erosions are increasing operators, i.e.,

$$f \leq g \implies \delta(f) \leq \delta(g) \text{ and } \varepsilon(f) \leq \varepsilon(g).$$

3.3 Metric dilation and erosion on $\bar{\mathcal{L}}_m$

We introduce a flexible approach to define dilation and erosion on $\mathcal{F}(X,\overline{\mathbb{R}})$ which allow us to characterize the dilation and erosion of m-continuous functions.

Hypograph and epigraph of a function. Given a function $f \in \mathcal{F}(X,\overline{\mathbb{R}})$, we define it hypograph $U(f)$, also known as umbra in the mathematical morphology literature, and its epigraph $U^c(f)$ as follows

$$\begin{aligned} U(f) &= \{(y,a) \,:\, y \in X,\, a \in \mathbb{R},\ \text{such that } a \leq f(y)\} \\ U^c(f) &= \{(y,a) \,:\, y \in X,\, a \in \mathbb{R},\ \text{such that } a \geq f(y)\}. \end{aligned}$$

Structuring functions and dilation on $\mathcal{F}(X,\overline{\mathbb{R}})$. A spatially-variant structuring function w on X is a map $w : X^2 \to \overline{\mathbb{R}}$; such a function w has a dual $\breve{w}$ defined by transposition, i.e., $\breve{w}(x,y) = w(y,x)$, and to every point $x \in X$ it associates two functions $w_x, \breve{w}_x : X \to \overline{\mathbb{R}}$ defined by $w_x = w(x,y)$ and $\breve{w}_x = w(y,x)$.

The dilation δ_w and erosion ε_w by the spatially-variant structuring function w of $f \in \mathcal{F}(X,\overline{\mathbb{R}})$ are the operators $\mathcal{F}(X,\overline{\mathbb{R}}) \to \mathcal{F}(X,\overline{\mathbb{R}})$ defined as

$$\begin{aligned} \delta_w(f)(x) &= \sup_{(y,a)\in U(f)} \{a + w(y,x)\}, \\ \varepsilon_w(f)(x) &= \inf_{(y,a)\in U^c(f)} \{a - \breve{w}(y,x)\}, \\ &= \inf_{(y,a)\in U^c(f)} \{a - w(x,y)\}, \end{aligned} \tag{22}$$

which gives

$$\begin{cases} \delta_w(f)(x) = \sup_{y\in X} \{f(y) + w(y,x)\}, \\ \\ \varepsilon_w(f)(x) = \inf_{y\in X} \{f(y) - w(x,y)\}. \end{cases} \tag{23}$$

It is used the further convention that expression $\inf - \inf$ gives $-\infty$ for $\delta_w(f)$ and $+\infty$ for $\varepsilon_w(f)$. A notably particular case of operators (23) occurs with translation invariant structuring function w. Here X is an abelian additive group with the neutral element o, then for any x, w_x is the translate of w_o by x, with $w_x = (x,y) = w(o, y-x)$. Note that $w_o = w(o,x)$ is just the structuring function b in (1).

It is easily shown from (22) that δ_w and ε_w commute with intensity shift $f \mapsto f + a$, $a \in \mathbb{R}$.

Proposition 7 *For any spatially-variant structuring function w, the pair $(\delta_w, \varepsilon_w)$ is an adjunction on $\mathcal{F}(X, \overline{\mathbb{R}})$.*

Proof. The classical proof can be given using expression (23), but then we have to take special care of infinity terms. Let us follow the proof proposed in [34]. For any $f, g \in \mathcal{F}(X, \overline{\mathbb{R}})$, we have the equivalence

$$\begin{array}{rcl} f \leq g & \Leftrightarrow & \forall (y,a) \in U(f), \\ a \leq g(y) & \Leftrightarrow & \forall (y,a) \in U^c(g),\ f(y) \leq a. \end{array} \tag{24}$$

Let $f, g \in \mathcal{F}(X, \overline{\mathbb{R}})$. The following statements are equivalent:

$$\begin{array}{rcl} \delta_w(f) & \leq & g \\ \delta_w(f)(x) & \leq & b,\ \forall (x,b) \in U^c(g)\ \text{(using (24))} \\ \sup\limits_{(y,a)\in U(f)} \{w(y,x) + a\} & \leq & b,\ \forall (x,b) \in U^c(g)\ \text{(using (22))} \\ (w(y,x) + a) & \leq & b,\ \forall (x,b) \in U^c(g),\ \forall (y,a) \in U(f) \\ a & \leq & (b - w(y,x)),\ \forall (y,a) \in U(f),\ \forall (x,b) \in U^c(g) \\ a & \leq & \inf\limits_{(x,b)\in U^c(g)} \{b - w(y,x)\},\ \forall (y,a) \in U(f) \\ a & \leq & \varepsilon_w(g)(y),\ \forall (y,a) \in U(f)\ \text{(using (24))} \\ f & \leq & \varepsilon_w(g)\ \text{(using (24))} \end{array}$$

Hence $\delta_w(f) \leq g \Leftrightarrow f \leq \varepsilon_w(g)$, and so we have an adjunction by definition. ■

Adjuntion induces a duality between dilation an erosion. Moreover, dilation and erosion by spatially-variant structuring functions are linked by the duality associated to the negative (or inversion) $f \mapsto -f$ of $\mathcal{F}(X, \overline{\mathbb{R}})$.

Proposition 8 *For any spatially-variant structuring function w and for $f \in \mathcal{F}(X, \overline{\mathbb{R}})$, we have*

$$\begin{aligned} -\delta_w(-f) &= \varepsilon_{\breve{w}}(f) \\ -\varepsilon_w(-f) &= \delta_{\breve{w}}(f). \end{aligned}$$

Proof. Here, again another proof can be derived using expression (23), taking special care of infinity terms. Let us follow the proof proposed in [34].

To verify the first equality, we note first that for $b = -a$, $(y, a) \in U(f)$ if and only if $(y, b) \in U^c(f)$; hence, from (22) one has for all $x \in X$

$$\begin{aligned} -\delta_w(-f) &= -\sup_{(y,a)\in U(-f)} \{a + w(y, x)\} \\ &= \inf_{(y,a)\in U(-f)} -\{a + w(y, x)\} \\ &= \inf_{(y,b)\in U^c(f)} \{b - w(y, x)\} \\ &= \inf_{(y,b)\in U^c(f)} \{b - \breve{w}(x, y)\} = \varepsilon_{\breve{w}}(f). \end{aligned}$$

The second equality can be derived from the first, by taking f and $\breve{w}$ instead of f and w. ■

Structuring functions and dilation on $\bar{\mathcal{L}}_m$. In this general setting, it can be proven that for any function $f \in \mathcal{F}(X, \overline{\mathbb{R}})$, if for any $x \in X$ the spatially-variant structuring function w_x is Lipschitz, then both the dilation $\delta_w(f)$ and the erosion $\varepsilon_w(f)$ are Lipschitz functions [34]. The proof is easy since the dilation (resp. erosion) can be seem as the supremum (resp. infimum) of translated w_x (Lipschitz functions) on $X \times \overline{\mathbb{R}}$, which therefore is Lipschitz.

Let us provide more complete results on $\bar{\mathcal{L}}_m$ for morphological operators on m-continuous functions, and first we consider the case of flat spatially-variant structuring functions. Every flat dilation or erosion is characterized by a structuring element mapping $W : X \to \mathcal{K}'$ that associates a non empty compact set to each point in X. We denote by W_x the set associated to point $x \in X$. Let us consider the Hausdorff distance between two sets A and A':

$$H_\rho(A, A') = \inf \left\{\rho \,:\, A \subseteq A' \oplus B_\rho,\ A' \subseteq A \oplus B_\rho\right\},\ \ A, A' \in \mathcal{P}(X). \tag{25}$$

Theorem 9 (Serra, 1994 [42]) *Let us assume that the family of spatially-variant structuring elements satisfies*

$$H_\rho(W_x, W_y) \leq d(x, y)$$

Then, every supremum, infimum and composition product of dilations or erosions by the family structuring elements applies $\bar{\mathcal{L}}_m$ on itself and is continuous.

In order to be more general with respect to the structuring function w, we need to extend the notion of Hausdorff distance to functions. Let us denote by $\delta_{\mathrm{Cyl}_{\rho,k}}(g)$ the dilation of

function g by a circular cylinder of radius ρ and height $k\rho$, i.e.,

$$\delta_{\mathrm{Cyl}_{\rho,k}}(g)(x) = \sup_{y \in B_\rho(x)} \{g(y)\} + k\rho$$

Then, the quantity $h : \mathcal{F}(X, \overline{\mathbb{R}}) \times \mathcal{F}(X, \overline{\mathbb{R}}) \to \mathbb{R}_+$

$$h(g, g') = \inf \left\{ \rho \ : \ g \leq \delta_{\mathrm{Cyl}_{\rho,k}}(g'),\ g' \leq \delta_{\mathrm{Cyl}_{\rho,k}}(g) \right\},\ \ g, g' \in \mathcal{F}(X, \overline{\mathbb{R}}). \tag{26}$$

is a Hausdorff type distance on $\mathcal{F}(X, \overline{\mathbb{R}})$ [41, 43]. The appearance of a coefficient $k > 0$ is a consequence of dimensionality requirements since we are working in the product space $X \times \overline{\mathbb{R}}$ and it measures the ratio between the units of the physical space X and the intensity space $\overline{\mathbb{R}}$. It is therefore a free parameter.

In order to have the properties of a distance, specifically the fact that $h(g, g') = 0$ implies $g = g'$ we need to restrict ourselves to the class of compact functions of $\mathcal{F}(X, \overline{\mathbb{R}})$, denoted by $\Phi_C((X, \overline{\mathbb{R}}))$. Namely, a function $f \in \Phi_C((X, \overline{\mathbb{R}}))$ satisfies [40]:

- f is upper semi-continuous, i.e., its upper level set of f

  $$X_a^+(f) = \{x \in X \ : \ f(x) \geq a\},$$

  are compact sets for all $a \in \overline{\mathbb{R}} \setminus -\infty$;

- f is upper bounded and its strict support $\mathrm{supp}(f)$ is compact in X, i.e.,

  $$\mathrm{supp}(f) = \{x \in X \ : \ f(x) \neq -\infty\} \text{ is compact and not empty.}$$

Then, the set $\tilde{U}(f)$ of $X \times \mathbb{R}$ defined

$$\tilde{U}(f) \ \ = \ \ \{(y, a) \ : \ y \in \mathrm{supp}(f),\ a \in \mathbb{R},\ \text{ such that } \ \min(f) \leq a \leq f(y)\},$$

where $\min(f) = \inf\{f(x) \ : \ f(x) \neq -\infty\}$, is compact.

We introduce now the following rather general result.

Theorem 10 (Serra, 1997 [43]) *Let us consider the dilation δ_w on the lattice $\mathcal{F}(X, \overline{\mathbb{R}})$, with structuring functions w, $w_x \in\in \Phi_C((X, \overline{\mathbb{R}}))$ and modulus of continity m' with respect to Hausdorff distance* (26)*, i.e.,*

$$h(w_x, w_y) \leq m'\left(d(x, y)\right).$$

Given $f \in \bar{\mathcal{L}}_m$, then dilation δ_w maps the sublattice $\bar{\mathcal{L}}_m$ into the sublattice $\bar{\mathcal{L}}_{(m+k)\circ m'}$.

Any infimum of dilations which have the same modulus m' also provides $(m + k) \circ m'$-continuous functions. By duality, a similar result result is obtained by erosions $\varepsilon_w(f)$ and supremum of erosion having the same modulus of continuity.

Proof. Let $f \in \bar{\mathcal{L}}_m$. Put $h(w_x, w_y) = h$. At point y, we have

$$\delta_w(f)(y) = \sup\{f(z) + w_y(z),\ z \in X\}.$$

But

$$w_y(z) \leq \delta_{\mathrm{Cyl}_{h,k}}(w_x)(z) = \sup\{w_x(u),\ :\ u \in B_h(z)\} + kh$$

and

$$f(z) \leq f(u) + m\left(d(z,u)\right).$$

Hence, we have

$$\begin{aligned} \delta_w(f)(y) &\leq \sup\{f(u) + w_x(u) + m\left(d(z,u)\right),\ z \in B_h(u)\} + kh \\ &\leq \sup\{f(u) + w_x(u),\ u \in X\} + m\left(h\right) + kh \end{aligned}$$

so

$$\delta_w(f)(y) \leq \delta_w(f)(x) + m(h) + kh,$$

and the similar inequality by interverting x and y. Finally

$$|\delta_w(f)(x) - \delta_w(f)(y)| \leq m(h) + k(h) \leq (m+k) \circ m'\left(d(x,y)\right).$$

■

In the flat case with compact structuring elements $\{W_x,\ x \in X\}$, one has

$$w_x(z) = \begin{cases} 0 & \text{if } z \in W_x \\ -\infty & \text{if } z \notin W_x \end{cases}$$

which implies as condition $h(w_x, w_y) = H(W_x, W_y) \leq m'\left(d(x,y)\right)$. In that case, theorem 10 proves that any m-continuous function is transformed by flat dilation or erosion into a $m \circ m'$-continuous one. When $m' \leq \mathrm{Id}$, we recover Theorem 9 and the flat dilation and erosion maps $\mathcal{L}_m$ into itself. This situation corresponds to the classical translation invariant flat morphology, i.e., $W_x = W_o + x$, $x \in X$.

The latter particular case is extended to the case of classical functional dilation and erosion (1), where X is affine, e.g., $\mathbb{R}^n$, and one takes for structuring function w_x the translate by vector x of the structuring function x defined at the origin. Then $h(w_x, w_y) = d(x,y)$, so $m' = \mathrm{Id}$ and thus $(m+k) \circ m' = m$. Operators (1) preserve all equicontinuous lattices $\mathcal{L}_m$.

Discrete spaces. When X and $\overline{\mathbb{R}}$ are sampled by means of regular grids, the previous operations can be arbitrary approximated by their digital versions, as a consequence of the continuity.

Random functions.

3.4 Equicontinuous modulus estimation using morphological operators

The modulus of continuity for an equicontinuous function f satisfies

$$m_f(h) = \sup\left\{|f(x) - f(y)| \,:\, x, y \in X,\, d(x,y) \leq h\right\}. \tag{27}$$

This measurement of the maximum variation of f can be compared to the variogram of the function:

$$\gamma_f(h) = \mathbb{E}\left\{(f(x) - f(y))^2 \,:\, x, y \in X,\, d(x,y) \leq h\right\}, \tag{28}$$

which provides the quadratic mean of the variation of f between the points. In the case of fractional Brownian motion of Hurst parameter H, the variogram can be written as [45]: $\gamma_f(h) \propto h^{2H}$.

The modulus $m_f(h)$ turns out to be a meaningful descriptor which have been used for morphological local sampling of images as follows [42]. The idea is to first compute a local version of the modulus of f at x:

$$m_f(h, x) = \sup\left\{(\delta_{B_h}(f) - f)(x),\, (f - \varepsilon_{B_h}(f))(x)\right\},$$

where B_h is a ball of radius h. Second, consider the so-called inverse $h_f(m, x)$ of $m_f(h, x)$: the value of $h_f(m, x)$ is the size of the minimum ball centred at x such that local variation is $\leq m_f(h, x)$. Using this function, the goal is to construct a grid whose variable spacing fits with function h.

We note that an alternative way to compute the local modulus of continuity of f would be linked to the morphological gradient by structuring element B_h:

$$m_f(h, x) = \{\delta_{B_h}(f)(x) - \varepsilon_{B_h}(f)(x)\} = \beta_{B_h}(f)(x). \tag{29}$$

4 Morphological semigroups on length spaces

A natural choice of a spatially-variant structuring function can be the distance function and therefore $w(x, y) = w(y, x) = -d(x, y)$. If $X = \mathbb{R}^n$, one has $w(y, x) = -\|x - y\|$, i.e., the dilation becomes as expected $\delta_w(f)(x) = \sup_{y \in X}\{f(y) - \|x - y\|\}$. This case and its role in Lipschitz regularization was widely studied in [34].

Let us consider a more rich family of structuring functions on metric space (X, d) which will lead to morphological semigroups on X, when X is a length space [3]. We assume an equicontinuous function $f : X \to \mathbb{R}$, $f \in \mathcal{L}_m$. Let us consider a one-dimensional (shape) function $L : \mathbb{R}_+ \to \mathbb{R}_+$, being increasing, superlinear, convex of class $\mathcal{C}^1$ such that $L(0) = 0$. For all scales $t > 0$, we define the dilation $D_{L;\,t}f$ and the erosion $E_{L;\,t}f$ operators of f on (X, d) according to L as follows

$$D_{L;\,t}f(x) = \sup_{y \in X}\left\{f(y) - tL\left(\frac{d(x,y)}{t}\right)\right\}, \quad \forall x \in X, \tag{30}$$

$$E_{L;\,t}f(x) = \inf_{y \in X}\left\{f(y) + tL\left(\frac{d(x,y)}{t}\right)\right\}, \quad \forall x \in X. \tag{31}$$

We adopt the convention $D_{L;\,0}f = E_{L;\,0}f = f$. We notice that these operators are just the case of (23) with symmetric structuring function:

$$w(x,y) = -tL\left(\frac{d(x,y)}{t}\right).$$

A typical example of a shape function is $L(q) = q^P/P$, $P > 1$, such that

$$w_{P,t}(x,y) = -\frac{d(x,y)^P}{Pt^{P-1}}.$$

Properties. The following properties hold for any metric space (X,d).

1. (Adjunction) For any two real-valued functions f and g on (X,d), the pair $(E_{L;\,t}, D_{L;\,t})$ forms an adjunction, i.e.,

$$D_{L;\,t}f(x) \le g(x) \Leftrightarrow f(x) \le E_{L;\,t}g(x), \quad \forall x \in X.$$

2. (Duality by involution) For any function f and $\forall x \in X$, one has

$$D_{L;\,t}f(x) = -E_{L;\,t}(-f)(x); \text{ and } E_{L;\,t}f(x) = -D_{L;\,t}(-f)(x), \ \forall t > 0.$$

3. (Increaseness) If $f(x) \le g(x)$, $\forall x \in X$, then

$$D_{L;\,t}f(x) \le D_{L;\,t}g(x); \text{ and } E_{L;\,t}f(x) \le E_{L;\,t}g(x), \ \forall x \in X, \forall t > 0.$$

4. (Extensivity and anti-extensivity)

$$D_{L;\,t}f(x) \ge f(x); \text{ and } E_{L;\,t}f(x) \le f(x), \ \forall x \in X, \forall t > 0.$$

5. (Ordering property) If $0 < s < t$ then $\forall x \in X$

$$\inf_X f \le E_{L;\,t}f(x) \le E_{L;\,s}f(x) \le f(x) \le D_{L;\,s}f(x) \le D_{L;\,t}f(x) \le \sup_X f.$$

6. (Convergence) For any function f and $\forall x \in X$, $D_{L;\,t}f(x)$ and $E_{L;\,t}f(x)$ converge monotonically to $f(x)$ as $t \to 0$. In particular $\lim_{t\to 0} D_{L;\,t}f = f$ and $\lim_{t\to 0} E_{L;\,t}f = f$.

7. (Semigroup) For any function f and $\forall x \in X$, and for all pair of scales $s, t > 0$,

   - If X is metric space:

$$D_{L;\,t}D_{L;\,s}f \le D_{L;\,t+s}f; \text{ and } E_{L;\,t}E_{L;\,s}f \ge E_{L;\,t+s}f.$$

   - If X is a length space:

$$D_{L;\,t}D_{L;\,s}f = D_{L;\,t+s}f; \text{ and } E_{L;\,t}E_{L;\,s}f = E_{L;\,t+s}f.$$

The proof for the semigroup in length spaces is important since justifies the need of geodesics in X, which will be important for the sequel. Following Gromov [19], a length space is a metric space (X, d) such that for any pair of points $x, y \in X$, we have $d(x, y) = \inf\{\text{Length}(\sigma)\}$, where the infimum is taken over all rectifiable curves $\sigma : [0, 1] \to X$ connecting x with y, i.e., $\sigma(0) = x$ and $\sigma(1) = y$. Note that every geodesic space is a length space. For the converse, we have the Hopf–Rinow Theorem: Let X be a length space, complete and locally compact, then X is a geodesic space.

Let us state the semigroup property proof. For the sake of simplicity the case of the canonic shape function $L(q) = q^2/2$. Now, triangle inequality implies that for all $x, y \in X$ and $s, t > 0$,

$$\frac{d(x,y)^2}{2(t+s)} \leq \inf_{z \in X} \left[\frac{d(x,z)^2}{2t} + \frac{d(z,y)^2}{2s} \right]. \tag{32}$$

The equality in (32) in length spaces comes from choosing a minimal geodesic between x and y, and a point z on this geodesic with $d(x, z) = \frac{t}{s+t}\, d(x, y)$. Finally, from (32), we obtain

$$\begin{aligned} E_{L;\, t+s} f(x) &= \inf_{y \in X} \left[f(y) + \frac{d(x,y)^2}{2(t+s)} \right] = \inf_{y \in X} \inf_{z \in X} \left[f(y) + \frac{d(x,z)^2}{2t} + \frac{d(z,y)^2}{2s} \right] \\ &= E_{L;\, t} E_{L;\, s} f(x). \end{aligned}$$

Morphological PDE on metric spaces. The rationale behind the choice of the notation $L(q)$ as Lagrangian for the structuring function is the fact that there is a connection with the classical theory of Hamilton–Jacobi PDEs.

The morphological PDE on a length space (X, d) is the following initial-value Hamilton–Jacobi first-order equation [3]:

$$\begin{cases} \frac{\partial}{\partial t} u(x,t) \pm H\left(|\nabla^- u(x,t)|\right) = 0, & \text{in } X \times (0, +\infty), \\ \\ u(x, 0) = f(x), & \text{in } X, \end{cases} \tag{33}$$

where the initial condition $f : X \to \mathbb{R}$ is a continuous bounded function and $H : \mathbb{R}_+ \to \mathbb{R}_+$ is the Legendre transform of function $L(q)$:

$$H(p) = \max_{q \in \mathbb{R}_+} \{pq - L(q)\}, \;\; p \in \mathbb{R}_+.$$

Then, the solutions of PDE problem (33) are the dilation (30) and erosion (31) semigroups [3]:

$$u(x,t) = D_{L;\, t} f(x) \;\; (\text{for} - \text{sign}), \tag{34}$$

$$u(x,t) = E_{L;\, t} f(x) \;\; (\text{for} + \text{sign}). \tag{35}$$

The solutions hold for all $x \in X$ and for almost everywhere $t > 0$.

5 Fractal dimension, fractal functions and mathematical morphology

In this section we consider the notion of fractal function as a model for non-smooth signal and images as well as the classical methods from mathematical morphology to estimate the fractal dimension of those functions.

5.1 From fractal dimension to fractal functions

Let us review the basic notions on fractal functions, for more details [25].

Fractal dimensions and fractal sets. The *Hausdorff dimension* [15], also known as Hausdorff–Besicovitch dimension, is a measure of roughness, or more specifically, fractal dimension of a set. Qualitatively, for smooth sets, i.e., a shape having small number of corners, the Hausdorff dimension is an integer agreeing with the topological dimension. Fractals present properties of scaling and self-similarity and they have non-integer Hausdorff dimensions which strictly exceeds its topological dimension. The Hausdorff dimension measures in fact the local size of a space taking into account the metric distance between points. Consider the number $N(\epsilon)$ of balls of radius at most ϵ required to cover the set completely. When ϵ is very small, $N(\epsilon)$ grows polynomially with $1/\epsilon$. For a sufficiently well-behaved set, the Hausdorff dimension is the unique number d such that $N(\epsilon)$ grows as $1/\epsilon^d$ as ϵ approaches zero. Formaly, let X be a metric space. If $S \subset X$ and $d \in [0, +\infty)$, the d-dimensional Hausdorff outer measure of S is defined as

$$\mathcal{H}^d(S) = \lim_{r \to 0} \inf \Big\{ \sum_i r_i^d : \text{ there is a cover of } S \text{ by balls with radii } 0 < r_i < r \Big\}.$$

The Hausdorff dimension of S is then defined by

$$\dim_{\mathrm{H}}(S) = \inf\{d \geq 0 : \mathcal{H}^d(S) = 0\}.$$

Countable sets have Hausdorff dimension 0. The Euclidean space $\mathbb{R}^n$ has Hausdorff dimension n, and the circle $\mathbb{S}^1$ has Hausdorff dimension 1. As an example of fractal set, we can consider the Cantor set: a zero-dimensional topological space (which turn out to be an ultrametric space), is a union of two copies of itself, each copy shrunk by a factor 1/3. It can be shown that its Hausdorff dimension is $\log(2)/\log(3) \approx 0.63$, see for instance [29].

The *Minkowski-–Bouligand dimension* [33, 5], also known as box-counting dimension, is a way of determining the fractal dimension of a set $S \subset X$ in a metric space X as follows.

First, let us consider set S is on an evenly spaced grid. Then, count how many boxes are required to cover the set. The box-counting dimension is calculated by seeing how this number changes as we make the grid finer by applying a box-counting algorithm. More

precisely, suppose that N_ϵ is the number of boxes of side length ϵ required to cover the set. Then the box-counting dimension is defined as

$$\dim_{\text{box}}(S) = \lim_{\epsilon \to 0} \frac{\log N(\epsilon)}{\log(1/\epsilon)}.$$

This implies that $N(\epsilon)$ displays an approximate power law with respect to the scale: $N(\epsilon) \sim \epsilon^{-\dim_{\text{box}}(S)}$.

Instead of boxes, the advantage of using balls B_r is that can be defined in any metric space. In that case, the Minkowski–Bouligand dimension is given by

$$\dim_{\text{M}}(S) = n - \lim_{\epsilon \to 0} \frac{\log \text{vol}(S_\epsilon)}{\log \epsilon} = \lim_{\epsilon \to 0} \frac{\log \left[\text{vol}(S_\epsilon)/\epsilon^n\right]}{\log \left[1/\epsilon\right]},$$

where for each radius $\epsilon > 0$, the set S_ϵ is defined to be the ϵ-neighborhood of S, i.e. the set of all points in R^n which are at distance less than ϵ from S. Or equivalently, S_ϵ, called the Minkowski cover, is the union of all the open balls B_ϵ of radius ϵ which are centered at a point in S, i.e.,

$$S_\epsilon = S \oplus B_\epsilon. \tag{36}$$

In the case of a compact set $S \subset \mathbb{R}^n$, we have $\dim_{\text{box}}(S) = \dim_{\text{M}}(S)$. In general, for each compact subset of $\mathbb{R}^n$, one has [25]:

$$0 \leq \dim_{\text{H}}(S) \leq \dim_{\text{M}}(S) \leq n.$$

Because of the connection with Minkowski addition, in the sequel, we call fractal dimension of S, $\dim(S)$, the Minkowski–Bouligand dimension.

Fractal funtions. A real valued function $f : \mathbb{R}^n \to \mathbb{R}$ is called fractal if its graph

$$\text{Gr}(f) = ((x, a) \in \mathbb{R}^n \times \mathbb{R} \ : \ a = f(x)) \tag{37}$$

is a fractal set in $\mathbb{R}^{n+1}$. If f is continuous, then its graph is a continuous curve with topological dimension equal to n. Hence [29]:

$$f \text{ is continuous} \implies n \leq \dim_{\text{H}}(\text{Gr}(f)) \leq \dim_{\text{M}}(\text{Gr}(f)) \leq n + 1$$

Examples of fractal functions. Let us consider two of the most classic examples of parametric fractal functions [25].

- **Weierstrass function.** The function was initally defined as a Fourier series: $W(x) = \sum_{n=0}^{\infty} a^n \cos(b^n \pi x)$, where $0 < a < 1$, b is a positive odd integer, and $ab > 1 + 3/2\pi$. The minimum value of b for which there exists $0 < a < 1$ such that these constraints are satisfied is $b = 7$.

An alternative way to write the Weierstrass function is

$$W_\alpha(x) = \sum_{n=0}^{\infty} b^{-n\alpha} \cos(b^n \pi x), \;\; b > 0, \; 0 < \alpha < 1, \tag{38}$$

with $\alpha = -\frac{\log(a)}{\log(b)}$. If b is integer, W_α is periodic.

The function $W_\alpha(x)$ is an example of a real-valued function that is continuous everywhere but differentiable nowhere. Indeed, its derivative, $W'_\alpha(x) = \pi \sum_{n=0}^{\infty} \beta^n \sin(b^n \pi x)$, diverges since $\beta = b^{1-\alpha} > 1$.

Then $W_\alpha(x)$ is Hölder continuous of exponent α. It is an example of a fractal curve of dimension [44]: $\dim_{\mathrm{H}} = \dim_{\mathrm{M}} = 2 - \alpha$.

- **Fractional Brownian motion.** The fractional Brownian motion (fBm) [24], also called a fractal Brownian motion, is a generalization of Brownian motion where the increments of fBm need not be independent. fBm is a continuous-time Gaussian process $B_H(t)$ on $[0, T]$, that starts at zero, has expectation zero for all t in $[0, T]$, and has the following covariance function:

$$\mathbb{E}[B_H(t) B_H(s)] = \tfrac{1}{2}(|t|^{2H} + |s|^{2H} - |t - s|^{2H}),$$

where $0 < H < 1$ is called the Hurst parameter associated with the fractional Brownian motion. The value of H determines what kind of process the fBm is: i) if $H = 1/2$ then the process is in fact a Brownian motion (Wiener process); ii) if $H > 1/2$ then the increments of the process are positively correlated; iii) if $H < 1/2$ then the increments of the process are negatively correlated.

Its power spectrum is [25] $S_H(\omega) \propto \|\omega\|^{-2H-1}$. Latter property can be used to simulate FBm signals via the FFT.

The process is self-similar, since in terms of probability distributions:

$$B_H(at) \sim |a|^H B_H(t).$$

This property is due to the fact that the covariance function is homogeneous of order $2H$ and can be considered as a fractal property. FBm can also be defined as the unique mean-zero Gaussian process, null at the origin, with stationary and self-similar increments $B_H(t) - B_H(s) \;\sim\; B_H(t - s)$.

Sample-paths are almost nowhere differentiable and almost-all trajectories are locally Hölder continuous of any order strictly less than H: for each such trajectory, for every $T > 0$ and for every $\epsilon > 0$ there exists a (random) constant c such that

$$|B_H(t) - B_H(s)| \leq c|t - s|^{H-\varepsilon}, \;\; \text{for } 0 < s, t < T.$$

With probability 1, the graph of $B_H(t)$ has $\dim_{\mathrm{H}} = \dim_{\mathrm{M}} = 2 - H$.

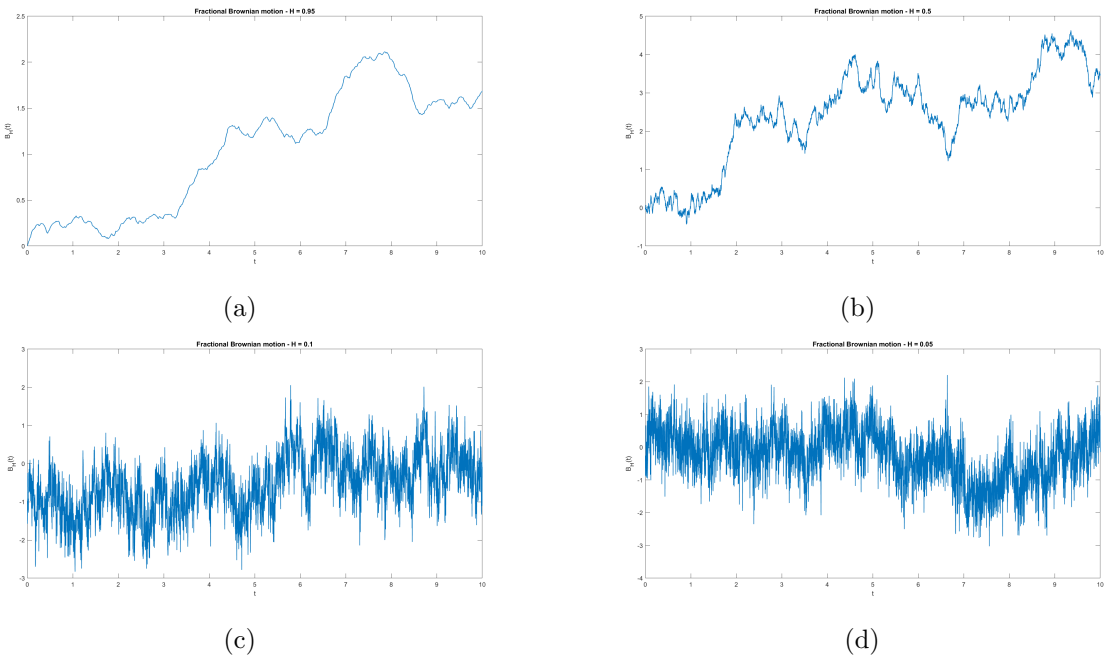

Figure 1: Examples of fractional Brownian motion sample-paths $B_H(t)$ for various values of Hurst parameter H, such that the fractal dimension is $\dim_{\mathrm{H}} = \dim_{\mathrm{M}} = 2 - H$: (a) $\dim_{\mathrm{M}} = 1.05$, (b) $\dim_{\mathrm{M}} = 1.50$, (c) $\dim_{\mathrm{M}} = 1.90$, (d) $\dim_{\mathrm{M}} = 1.95$.

Figure 1 depicts examples of fractional Brownian motion sample-paths $B_H(t)$ for four values of Hurst parameter $H = 0.95$, 0.50, 0.10 and 0.05. The fractal signals have been simulated using the MATLAB code [6] using the algorithm from [20].

Figure 2 illustrates three examples of the simulation of a fractional Brownian surface $B_H(x, y)$ on unit disk (column left) which can be also seen as 2D images (column right). Note that the covariance function is isotropic in (x, y). The simulation tool is again a MATLAB code [7] based on an algorithm from [20]. Thresholding a fractional Brownian image field provides a random set with fractal properties, see Figure 3.

As conclusion, we can say that in many cases the Hölder exponent is intimately related to the self-similarity exponent or dimension of fractals, hence resulting in a confusing identification of the three quantities. However, we should point out that self-similar processes and fractal curves or sets do not always possess a single Hölder exponent that can be related to the fractal dimension. For a mathematical treatement of the links between fractal dimension and Hölder exponent, the reader is referred to [9].

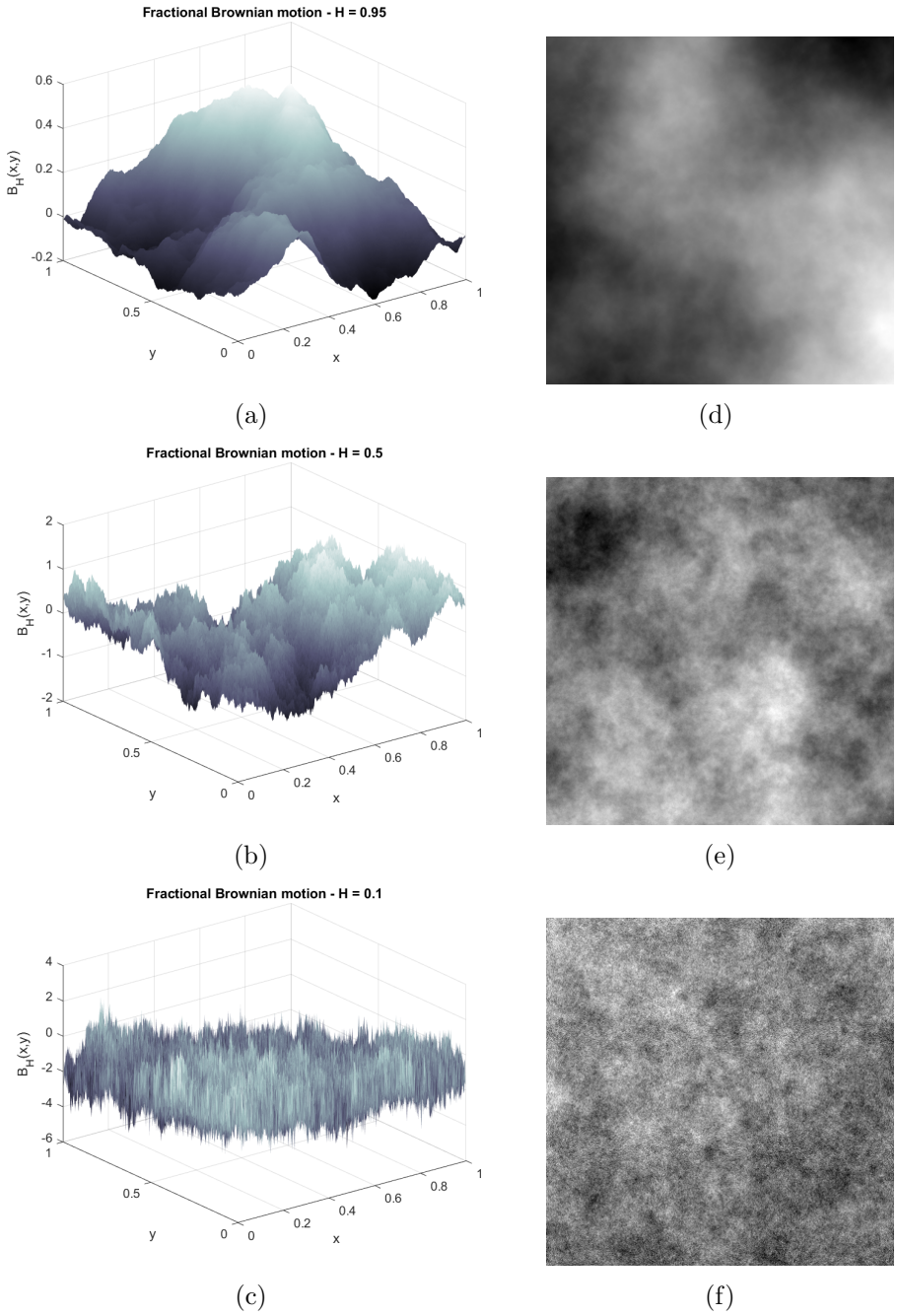

Figure 2: Left column, examples of fractional Brownian sample-surfaces $B_H((x, y))$ for various values of Hurst parameter H, such that the fractal dimension is $\dim_{\mathrm{H}} = \dim_{\mathrm{M}} = 3 - H$: (a) $\dim_{\mathrm{M}} = 2.05$, (b) $\dim_{\mathrm{M}} = 2.50$, (c) $\dim_{\mathrm{M}} = 2.90$. Right column, corresponding 2D image fields: (d) $\dim_{\mathrm{M}} = 2.05$, (e) $\dim_{\mathrm{M}} = 2.50$, (f) $\dim_{\mathrm{M}} = 2.90$.

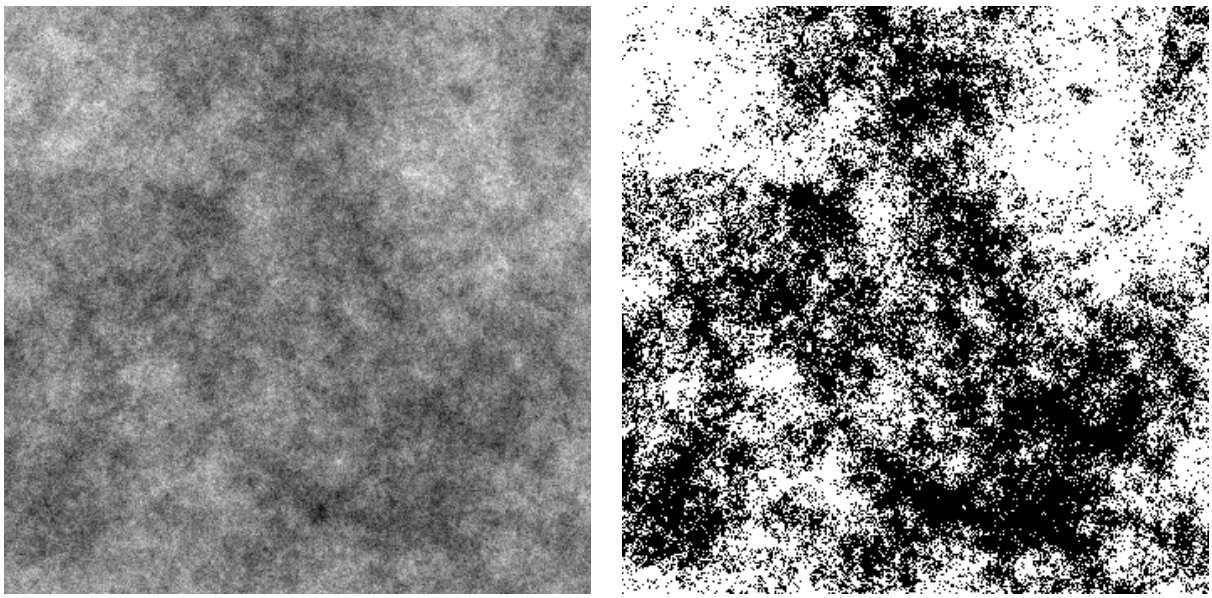

(a) (b)

Figure 3: (a) From realization of fractional Brownian field $B_H((x, y))$ with $H = 0.10$ to (b) realization of fractal set.

5.2 Classical fractal analysis using morphological operators on Euclidean space

The use of morphological operators as an alternative to wavelets for the estimation of fractal dimension from signals and images is well knwon, see for instance [36, 28]. See also [46, 10] for the 1D case. In this section, we mainly follow the overview papers [29, 45].

Multiscale operators are indeed naturally adapted to estimate the fractal dimension $\dim(S)$ since the Minkowski cover (36) is just the dilation of of S by the homothetic ϵB of B at scale ϵ, which can be generalized to any structuring element B and define the notion of morphological cover [29]:

$$C_\epsilon(S, B) = S \oplus \epsilon B.$$

The covering blanket method extends this principle to function graphs or intensity surfaces. Each point of the surface $\mathrm{Gr}(f)$ is replaced by a sphere B_ϵ of radius ϵ:

$$C_\epsilon(f, B) = \mathrm{Gr}(f) \oplus \epsilon B.$$

We introduce also the notion of upper and lower envelope of the morphological set cover of

$f \in \mathcal{F}(\mathbb{R}^n, \mathbb{R})$:

$$\begin{aligned} \mathrm{Upper}_\epsilon(f, B) &= \sup\{a \,:\, (x,a) \in C_\epsilon(f,B)\}, \\ \mathrm{Lower}_\epsilon(f, B) &= \inf\{a \,:\, (x,a) \in C_\epsilon(f,B)\}. \end{aligned} \tag{39}$$

In the case of a 2D function f, the area of the intensity surface $\mathrm{Gr}(f)$ is obtained by dividing the integral (volume) of the dilated surface by ϵ, with ϵ is small, i.e.,

$$\mathrm{area}_\epsilon(\mathrm{Gr}(f)) = \frac{\mathrm{vol}(\mathrm{Gr}(f) \oplus B_\epsilon)}{\epsilon} = \epsilon^{-1} \int_{\mathbb{R}^2} [(f \oplus B_\epsilon)(x) - (f \ominus B_\epsilon)(x)]\, dx.$$

We note that the volume of $\mathrm{Gr}(f) \oplus B_\epsilon$ corresponds to the integral of the gradient of f by B_ϵ [39]. Therefore, using the notion of morphological total variation (12), one has:

$$\mathrm{area}_\epsilon(\mathrm{Gr}(f)) = \lim_{\epsilon \to 0} \frac{MTV_{B_\epsilon}(f)}{\epsilon},$$

$$\mathrm{vol}_\epsilon(\mathrm{Gr}(f)) = \lim_{\epsilon \to 0} MTV_{B_\epsilon}(f).$$

Therefore for $f \in \mathcal{F}(\mathbb{R}^2, \mathbb{R})$, we have

$$\begin{aligned} \dim(\mathrm{Gr}(f)) &= 2 - \lim_{\epsilon \to 0} \frac{\log \mathrm{area}_\epsilon(\mathrm{Gr}(f))}{\log \epsilon} \\ &= 3 - \lim_{\epsilon \to 0} \frac{\log \mathrm{vol}(\mathrm{Gr}(f) \oplus B_\epsilon)}{\log \epsilon} = \lim_{\epsilon \to 0} \frac{\log\left[MTV_{B_\epsilon}(f)/\epsilon^3\right]}{\log[1/\epsilon]}. \end{aligned}$$

This result can be naturally generalized to functions on a n-dimensional space. Furthermore, instead of using $(n+1)$-dimensional structuring elements B, it is more consistent and more efficient from a computational viewpoint, to work on functional morphological operators.

Let us introduce the following ϵ-scaled structuring function $b_\epsilon : \mathbb{R}^n \to \mathbb{R}$ for any homothetic ϵB of the structuring element $B \subseteq \mathbb{R}^{n+1}$:

$$b_\epsilon(x) = \sup\{a \,:\, (x,a) \in \epsilon B,\ x \in \mathbb{R}^n,\ a \in \mathbb{R}\}. \tag{40}$$

Typical examples of symmetric structuring elements in the product space $\mathbb{R}^n \times \mathbb{R}$, proposed in [28, 29], are:

$$\begin{aligned} \epsilon B = \left\{(x,a) : \|x\|^2 + a^2 \le \epsilon\right\} &\implies b_\epsilon(x) = \sqrt{\epsilon - \|x\|^2},\ \|x\| \le \epsilon,\ \text{(spherical)} \\ \epsilon B = \{(x,a) : \|x\|_1 + |a| \le \epsilon\} &\implies b_\epsilon(x) = \epsilon - \|x\|_1,\ \|x\|_1 \le \epsilon,\ (L_1 \text{ hat}). \end{aligned}$$

Then we have the following result that we propose here in the case of a function $f \in \mathcal{F}(\mathbb{R}^n, \mathbb{R})$ (the original formulation in [28] is $n = 1$ and was extended to $n = 2$ in [29]).

Theorem 11 (Maragos and Sun, 1991) *Let $f : \Omega \subseteq \mathbb{R}^n \to \mathbb{R}$ be a continuous function. Let $B \subseteq \mathbb{R}^{n+1}$ be a compact set, single connected and symmetric in the product space $\mathbb{R}^n \times \mathbb{R}$. Then,*

$$\begin{aligned} Upper_\epsilon(f,B)(x) &= (f \oplus b_\epsilon)(x), \\ Lower_\epsilon(f,B)(x) &= (f \ominus b_\epsilon)(x). \end{aligned} \tag{41}$$

In addition, we have

$$vol(C_\epsilon(f,B)) = \int_\Omega [Upper_\epsilon(f,B)(x) - Lower_\epsilon(f,B)(x)]\, dx. \tag{42}$$

Thus, combining (41) *and* (42)*, one has*

$$vol(C_\epsilon(f,B)) = MTV_{b_\epsilon}(f),$$

and therefore the fractal dimension of

$$\dim(Gr(f)) = (n+1) - \lim_{\epsilon \to 0} \frac{\log MTV_{b_\epsilon}(f)}{\log \epsilon}. \tag{43}$$

Proof. We just need to proof (41) and (42). We follow [29].

Let $\mathrm{Spt}(b) = \{x \in \mathbb{R}^n : (x,a) \in B\}$. Since B is symmetric with respect to the product space, one has $b_\epsilon(x) = b_\epsilon(-x)$ and $\mathrm{Spt}(b) = \breve{\mathrm{Spt}}(b)$. Moreover, since B is symmetric with respect to intensity axis, $b_\epsilon(x) \geq 0$ for all x in its domain $\epsilon\mathrm{Spt}(b)$.

Let us denote

$$I(x) = \{c : (x,c) \in \epsilon B, : x \in \epsilon\mathrm{Spt}(b)\}.$$

Then note that

$$\begin{aligned} \sup\{c : c \in I(x)\} &= b_\epsilon(x), \\ \inf\{c : c \in I(x)\} &= -b_\epsilon(x). \end{aligned}$$

For (41), we have

$$\begin{aligned} \mathrm{Upper}_\epsilon(f,B)(x) &= \sup\{z : x = p + a,\ z = f(p) + c,\ (a,c) \in \epsilon B\}, \\ &= \sup\{f(x-a) + c : a \in \epsilon\mathrm{Spt}(b),\ c \in I(a)\}, \\ &= \sup\{f(p) + b_\epsilon(x-p) : x \in \epsilon\mathrm{Spt}(b) + p\}, \\ &= (f \oplus b_\epsilon)(x). \end{aligned}$$

A similar procedure can be used for $\mathrm{Lower}_\epsilon(f,B)(x)$.

Since $b_\epsilon(0) \geq 0$, it can be shown that

$$\mathrm{Upper}_\epsilon(f,B)(x) \geq f(x) \geq \mathrm{Lower}_\epsilon(f,B)(x),\ x \in \Omega$$

Define the set

$$Q(\epsilon) = \{(x,z) \,:\, x \in \Omega,\, \mathrm{Lower}_\epsilon(f,B)(x) \leq z \leq \mathrm{Upper}_\epsilon(f,B)(x)\}\,,$$

such that

$$\mathrm{vol}\,(Q(\epsilon)) = \int_\Omega [\mathrm{Upper}_\epsilon(f,B)(x) - \mathrm{Lower}_\epsilon(f,B)(x)]\,dx.$$

The goal is to prove that $Q(\epsilon) = C_\epsilon(f,B)$. First, let $(x,z) \in C_\epsilon(f,B)$. Then, $x \in \Omega$ and $(x,z) \in \mathrm{Gr}(f) \oplus \epsilon B$. Hence, $x = p + a$ and $z = f(x) + c$ for some $p \in \Omega$ and $(a,c) \in \epsilon B$. But then, from the definition of $\mathrm{Upper}_\epsilon(f,B)$, it follows that $z \leq \mathrm{Upper}_\epsilon(f,B)(x)$. Likewise, one gets $z \geq \mathrm{Lower}_\epsilon(f,B)(x)$. Therefore $(x,z) \in Q(\epsilon)$ and thus $C_\epsilon(f,B) \subset Q(\epsilon)$.

Now let $(x,z) \in Q(\epsilon)$. Define the set

$$\begin{aligned} K &= \epsilon B \cap \left[(\breve{\Omega} + x) \times (-\infty, +\infty)\right] \\ &= \left\{(a,c) \,:\, a \in \epsilon\mathrm{Spt}(b) \cap (\breve{\Omega} + x),\, c \in I(a).\right\} \end{aligned}$$

Then, K is a connected set. Define the function $\phi(a,c) = f(x-a) + c$ on K. The function ϕ is continuous and has a connected domain K. The value z lies between the maximum $\mathrm{Upper}_\epsilon(f,B)(x) = \sup_{\phi(a,c)\,:\,(a,c)\in K}$ and the minimum $\mathrm{Lower}_\epsilon(f,B)(x) = \inf_{\phi(a,c)\,:\,(a,c)\in K}$ value of ϕ on K. From Bolzano's intermediate value theorem, there is a point $(a',c') \in K$ such that $\phi(a',c') = z$. By setting $p = x - a'$ and $f(p) = z - c'$, we have $(p, f(p)) \in \mathrm{Gr}(f)$ and $(a',c') \in \epsilon B$. Hence $(x,z) \in C_\epsilon(f,B)$ and thus $Q(\epsilon) \subseteq C_\epsilon(f,B)$. Therefore $Q(\epsilon) = C_\epsilon(f,B)$

■

We note that B can be a flat structuring, like for instance a box of size w: $B = [-w,w]^n \times \{0\}$, in which case the corresponding structuring function is $b(x) = 0$ if $x \in [-w,w]^n$ and $b(x) = -\infty$ otherwise. In the 1D case, using as B the unit segment $[-1,1]^n \times \{0\}$, it corresponds to the case of [46, 10].

In practice, the fractal dimension is obtained from (43) by taking a structuring function b_ϵ, computing $MTV_{b_\epsilon}(f)$ for $\epsilon = 1, 2, ...$ and fitting a straight line using least squares of the graph $\log - \log$. The slope of this line give us $(n+1) - \dim(\mathrm{Gr}(f))$.

Let us illustrate the approach. For each experience, we have simulated 50 fractional Brownian surfaces $B_H(x,y)$ with a given value of H, such that $\dim_{\mathrm{M}} = 3 - H$, and considered a fractal image field f of 500×500 pixels from each realisation. See for instance the examples provided in Fig 2. We have considered three families of multiscale structuring functions b_ϵ: first, a flat diamond shape (rhomboid) defined in the support 3×3 pixels; second, a flat octagon in the support 7×7 pixels; third, an approximation to the sphere in the 3D support $5 \times 5 \times 5$ pixels. By flat, we mean that value the on the shape is 0 and $-\infty$ elsewhere. One can now compute the corresponding multiscale dilation and erosion.

We have computed the morphological total variation $MTV_{b_\epsilon}(f)$, with $\epsilon = 1, 2, \cdots, 100$ for the three cases. Figure 4(a) compares the $(\log\epsilon, \log MTV_{b_\epsilon}(f))$ curves from the same fractional Brownian image field of $\dim_{\mathrm{M}} = 2.6$ using three different multiscale structuring

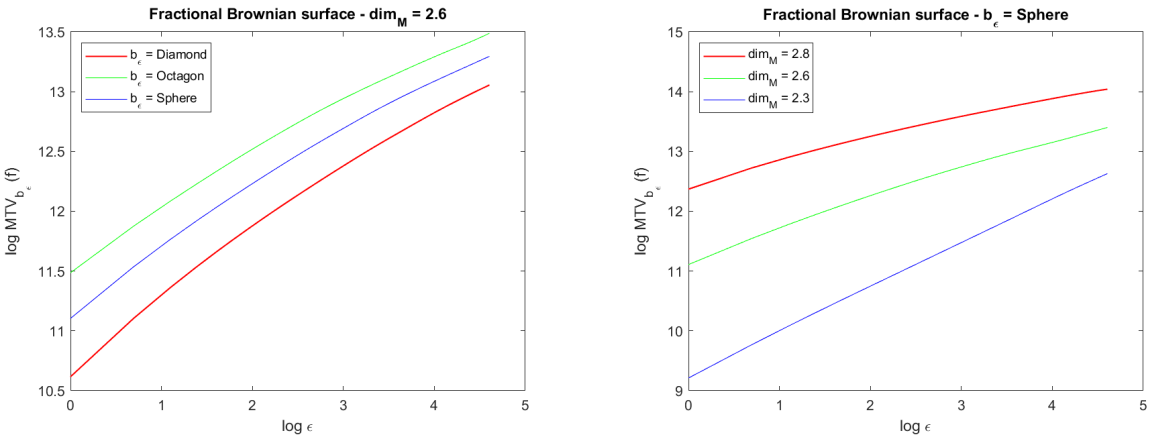

(a) (b)

Figure 4: Graphs in $\log - \log$ scale of $(\epsilon, MTV_{b_\epsilon}(f))$: (a) curves from the same fractional Brownian image field of $\dim_{\mathrm{M}} = 2.6$ using three different multiscale structuring functions b_ϵ; (b) curves using a spherical structuring function from three fractional Brownian images of different fractal dimension.

True	b_ϵ (diamond) (3×3)		b_ϵ (octagon) (7×7)		b_ϵ (spherical) (5×5×5)	
$\dim_M$	Mean ± StdDev	Error (%)	Mean ± StdDev	Error (%)	Mean ± StdDev	Error (%)
2.9	2.71 ± 0.01	6.2	2.79 ± 0.02	3.5	2.76 ± 0.01	4.7
2.8	2.64 ± 0.03	5.53	2.71 ± 0.02	2.8	2.68 ± 0.01	4.0
2.6	2.50 ± 0.02	3.5	2.59 ± 0.04	0.2	2.55 ± 0.03	1.8
2.5	2.44 ± 0.02	2.1	2.54 ± 0.04	1.7	2.49 ± 0.03	0.1
2.3	2.28 ± 0.03	0.5	2.38 ± 0.05	3.7	2.33 ± 0.04	1.3
2.1	2.14 ± 0.03	1.9	2.21 ± 0.05	5.3	2.17 ± 0.04	3.4

Table 1: Minkowski fractal dimension estimation from fractional Brownian image samples using morphological multiscale operators.

functions b_ϵ. As expected, we have almost straight lines of rather similar slope: the intercept depends of the structuring function. Figure 4(b) depicts the curves using a spherical structuring function, from three fractional Brownian images of different fractal dimension, which obviously produce different slopes.

Table 1 shows the estimated fractal dimension $\dim(\mathrm{Gr}(f))$, sample mean and standard deviation for 50 random realizations, and the percent estimation error $|\dim_{\mathrm{M}} - \dim(\mathrm{Gr}(f))|/\dim_{\mathrm{M}}$. The three families of structuring functions are compared. We should first emphasize that the fractal images we are working on are sampled version of non-bandlimited fractal function models and thus some degree of "fragmentation" is potentially lost during the sampling. In the classical approaches [29], it is suggested to have an infinitesimal shape as support for the structuring function, so typically the $3 \times 3 \times 3$ set of pixels around the origin. Our tests show that even with support set larger than this one, one still gets similar satisfying results. The rationale of the flat octagon or the sphere is to have a convex approximation to the unit ball better than the rhomboid one. In any case, the results obtained in these simulations are consistent with those reported previously for the morphological methods for fractal dimension estimation: Maragos in [29] mentioned an average error of about 3 to 4 % in the case of fractional Brownian motion paths (1D signal).

5.3 Hölder exponent estimation and fractal analysis in max-plus mathematics

In [13, 14], it was shown how the Gondran's $(\min, +)$-wavelets allow a characterisation of Hölder functions. The following theorem provides the main result.

Theorem 12 (Gondran and Kenoufi, 2014 [13]) *Let us consider the following multiscale structuring functions, $\lambda > 0$,*

$$\begin{aligned} b_{P,\lambda}(x) &= -\frac{\|x\|^P}{P\lambda^P}, \ P > 1, \\ b_{\infty,\lambda}(x) &= \{0, \ \textit{if } \|x\| \leq \lambda, \ -\infty \ \textit{else}\}. \end{aligned}$$

(Global version). The function $f \in \mathcal{F}(\mathbb{R}^n, \overline{\mathbb{R}})$ is α-Hölder, $0 < \alpha \leq 1$, if and only if it exists a constant C such as for $\lambda > 0$, one has the following conditions

$$\beta_{b_{\infty,\lambda}}(f)(x) \leq C\lambda^\alpha \tag{44}$$

$$\beta_{b_{P,\lambda}}(f)(x) \leq C\lambda^{\frac{P\alpha}{P-\alpha}} \tag{45}$$

(Local version). The function $f \in \mathcal{F}(\mathbb{R}^n, \overline{\mathbb{R}})$ is α-Hölder at point x_0, $0 < \alpha \leq 1$, $x_0 \in \mathbb{R}^n$ if and only if it exists a constant C such as for $\lambda > 0$, one has the following conditions

$$\beta_{b_{\infty,\lambda}}(f)(x) \leq C\left(\lambda^\alpha + \|x - x_0\|^\alpha\right) \tag{46}$$

$$\beta_{b_{P,\lambda}}(f)(x) \leq C\left(\lambda^{\frac{P\alpha}{P-\alpha}} + \|x - x_0\|^\alpha\right) \tag{47}$$

Proof. Let us follow [13]. We start with the case of the flat structuring function $b_{\infty,\lambda}(x)$.

For the global case, let us assume that $\beta_{b_{\infty,\lambda}} \leq K\lambda^\alpha$. For x and y in $\mathbb{R}^n$, one can assume that $f(x) \geq f(y)$. Then, one has for $\lambda = \|x-y\|$,

$$\sup_{\|x-z\|\leq\lambda} f(z) \geq f(x) \geq f(y) \geq \inf_{\|x-z\|\leq\lambda} f(z),$$

this yields to

$$|f(x)-f(y)| \leq \beta_{b_{\infty,\lambda}}(f)(x) = \beta_{B_\lambda}(f)(x) \leq K\lambda^\alpha \leq K\|x-y\|^\alpha,$$

where

$$\begin{aligned}\beta_{B_\lambda}(f)(x) &= \delta_{B_\lambda}(f)(x) - \varepsilon_{B_\lambda}(f)(x)\\ &= \sup_{\|x-z\|\leq\lambda} f(z) - \inf_{\|x-z\|\leq\lambda} f(z).\end{aligned}$$

Conversely, let us assume that $|f(x)-f(y)| \leq K\|x-y\|^\alpha$. Let y_1 and y_2 be the two points such as

$$\begin{aligned}f(y_1) &= \sup_{\|x-z\|\leq\lambda} f(z)\\ f(y_2) &= \inf_{\|x-z\|\leq\lambda} f(z).\end{aligned}$$

Then, we have

$$\beta_{b_{\infty,\lambda}}(f)(x) = f(y_1) - f(y_2) = f(y_1) - f(y) + f(y) - f(y_2),$$

which yields to

$$\begin{aligned}\beta_{b_{\infty,\lambda}}(f)(x) &\leq |f(y_1)-f(y)| + |f(y)-f(y_2)|\\ &\leq 2K\lambda^\alpha.\end{aligned}$$

For the local case, the procedure is rather similar. Let us assume that, given x_0, f satisfies (46), $\forall x$. Let us consider $\lambda = \|x-x_0\|$ and $f(x) \geq f(x_0)$, one has

$$\sup_{\|x-x_0\|\leq\lambda} f(z) \geq f(x) \geq f(x_0) \geq \inf_{\|x-x_0\|\leq\lambda} f(z),$$

combining with the case $f(x) \leq f(x_0)$, we get

$$|f(x)-f(x_0)| \leq \beta_{b_{\infty,\lambda}}(f)(x) \leq 2C\|x-x_0\|^\alpha.$$

Conversely, we suppose now that f is α-Hölder with constant K for all x and consider y_1 and y_2, such as $f(y_1) = \sup_{\|x-x_0\|\leq\lambda} f(z)$ and $f(y_2) = \inf_{\|x-x_0\|\leq\lambda} f(z)$. Then, one has

$$\begin{aligned}\beta_{b_{\infty,\lambda}}(f)(x) &= f(y_1) - f(y_2) = |f(y_1)-f(x_0)| + |f(x_0)-f(y_2)|\\ &\leq K\left(\|y_1-x_0\|^\alpha + \|y_2-x_0\|^\alpha\right)\\ &\leq K\left(\|y_1-x\|^\alpha + \|x-x_0\|^\alpha + \|y_2-x\|^\alpha + \|x-x_0\|^\alpha\right)\\ &\leq 2K\left(\lambda^\alpha + \|x-x_0\|^\alpha\right).\end{aligned}$$

In the case of structuring function $b_{P,\lambda}$, $P > 1$, let us assume first that f satisfies $\beta_{b_{P,\lambda}}(f)(x) \leq C\lambda^{\frac{P\alpha}{P-\alpha}}$. We consider $x, y \in \mathbb{R}^n$ with $f(x) \geq f(y)$, the principle is to use the reconstruction formula (16) of f:

$$f(x) = \inf_{\substack{\lambda \in \mathbb{R}_+ \\ z \in \mathbb{R}^n}} \left\{ (f \oplus b_{P,\lambda})(f)(z) - b_P\left(\frac{x-z}{\lambda}\right) \right\},$$

and for $f(y)$ the simplified dual reconstruction (18):

$$f(y) = \sup_{\lambda \in \mathbb{R}_+} \left\{ (f \ominus b_{P,\lambda})(f)(y) \right\}.$$

Thus, one has

$$\begin{aligned} f(x) - f(y) &\leq \inf_{\lambda \in \mathbb{R}_+} \left\{ (f \oplus b_{P,\lambda})(f)(y) - b_P\left(\frac{x-y}{\lambda}\right) - (f \ominus b_{P,\lambda})(f)(y) \right\} \\ &\leq \inf_{\lambda \in \mathbb{R}_+} \left\{ C\lambda^{\frac{P\alpha}{P-\alpha}} - b_P\left(\frac{x-y}{\lambda}\right) \right\}. \end{aligned} \tag{48}$$

The optimization at scale λ on

$$f(x) - f(y) \leq \inf_{\lambda \in \mathbb{R}_+} \left\{ C\lambda^{\frac{P\alpha}{P-\alpha}} + \frac{\|x-y\|^P}{P\lambda^P} \right\},$$

so on $C\lambda^{\frac{p\alpha}{P-\alpha}} + P^{-1}\lambda^{-P}\|x-y\|^P$. Now, by considering $\lambda^{\frac{p\alpha}{P-\alpha}} = \|x-y\|^\alpha$ and thus $\lambda = \|x-y\|^{\frac{P-\alpha}{P}}$, one has

$$C\lambda^{\frac{p\alpha}{P-\alpha}} + P^{-1}\lambda^{-P}\|x-y\|^P = (C + P^{-1})\|x-y\|^\alpha,$$

and therefore

$$f(x) - f(y) \leq (C + P^{-1})\|x-y\|^\alpha.$$

Conversely, let us assume that f is α-Hölder for all $x, y \in \mathbb{R}^n$. Using the definition of the morphological gradient, one has

$$\begin{aligned} \beta_{b_{p,\lambda}}(f)(z) &= (f \oplus b_{P,\lambda})(f)(z) - (f \ominus b_{P,\lambda})(f)(z) \\ &= \sup_{x \in \mathbb{R}^n} \left\{ f(x) + b_P\left(\frac{z-x}{\lambda}\right) \right\} - \inf_{y \in \mathbb{R}^n} \left\{ f(y) - b_P\left(\frac{z-y}{\lambda}\right) \right\} \\ &= \sup_{x,y \in \mathbb{R}^n} \left\{ f(x) - f(y) + b_p\left(\frac{z-x}{\lambda}\right) + b_p\left(\frac{z-y}{\lambda}\right) \right\}. \end{aligned}$$

Using now the Hölder continuity,

$$\beta_{b_{p,\lambda}}(f)(z) \leq \sup_{x,y \in \mathbb{R}^n} \left\{ K\|x-y\|^\alpha - P^{-1}\lambda^{-P}\|x-z\|^P - P^{-1}\lambda^{-P}\|y-z\|^P \right\}.$$

By optimising in x and y, we obtain that

$$\beta_{b_{p,\lambda}}(f)(z) \quad \leq \quad C\lambda^{\frac{\alpha P}{P-\alpha}}.$$

For the local case, the procedure is rather similar. Let us first assume that f satisfies (47) and $f(x) \geq f(x_0)$ and we use again the reconstruction equations:

$$f(x) = \inf_{\substack{\lambda \in \mathbb{R}_+ \\ z \in \mathbb{R}^n}} \left\{ (f \oplus b_{P,\lambda})(f)(z) - b_P\left(\frac{x-z}{\lambda}\right) \right\},$$

and

$$f(x_0) = \sup_{\lambda \in \mathbb{R}_+} \left\{ (f \ominus b_{P,\lambda})(f)(x_0) \right\}.$$

Combining with the case $f(x) \geq f(x_0)$, one obtain:

$$\begin{aligned} |f(x) - f(x_0)| &\leq \inf_{\lambda \in \mathbb{R}_+} \left\{ (f \oplus b_{P,\lambda})(f)(x_0) - b_P\left(\frac{x-x_0}{\lambda}\right) - (f \ominus b_{P,\lambda})(f)(x_0) \right\} \\ &\leq \inf_{\lambda \in \mathbb{R}_+} \left\{ C\lambda^{\frac{P\alpha}{P-\alpha}} + C\|x-x_0\|^\alpha - b_P\left(\frac{x-x_0}{\lambda}\right) \right\}. \end{aligned} \tag{49}$$

Now, the optimization at scale λ on

$$|f(x) - f(y)| \quad \leq \quad \inf_{\lambda \in \mathbb{R}_+} \left\{ C\lambda^{\frac{P\alpha}{P-\alpha}} + \frac{\|x-x_0\|^P}{P\lambda^P} \right\} + C\|x-x_0\|^\alpha,$$

so on $C\lambda^{\frac{p\alpha}{P-\alpha}} + P^{-1}\lambda^{-P}\|x-x_0\|^P$. By considering $\lambda^{\frac{p\alpha}{P-\alpha}} = \|x-x_0\|^\alpha$ and thus $\lambda = \|x - x_0\|^{\frac{P-\alpha}{P}}$, one has

$$C\lambda^{\frac{p\alpha}{P-\alpha}} + P^{-1}\lambda^{-P}\|x-x_0\|^P + C\|x-x_0\|^\alpha = (2C + P^{-1})\|x-x_0\|^\alpha,$$

and therefore

$$|f(x) - f(y)| \quad \leq \quad (2C + P^{-1})\left(\|x-x_0\|^\alpha\right).$$

Conversely, let us assume that f is α-Hölder for all $x, y \in \mathbb{R}^n$. Using the definition of the morphological gradient, one has

$$\begin{aligned} \beta_{b_{p,\lambda}}(f)(z) &= (f \oplus b_{P,\lambda})(f)(z) - (f \ominus b_{P,\lambda})(f)(z) \\ &= \sup_{x \in \mathbb{R}^n} \left\{ f(x) + b_P\left(\frac{z-x}{\lambda}\right) \right\} - \inf_{y \in \mathbb{R}^n} \left\{ f(y) - b_P\left(\frac{z-y}{\lambda}\right) \right\} \\ &= \sup_{x,y \in \mathbb{R}^n} \left\{ f(x) - f(y) + b_p\left(\frac{z-x}{\lambda}\right) + b_p\left(\frac{z-y}{\lambda}\right) \right\}. \end{aligned}$$

Since

$$f(x) - f(y) = f(x) - f(x_0) + f(x_0) - f(y),$$

one deduces, using now Hölder continuity,

$$\begin{aligned}
\beta_{b_{p,\lambda}}(f)(z) &\leq \sup_{x,y\in\mathbb{R}^n} \left\{K\|x-x_0\|^\alpha + K\|y-x_0\|^\alpha - P^{-1}\lambda^{-P}\|x-z\|^P - P^{-1}\lambda^{-P}\|y-z\|^P\right\} \\
&\leq 2\sup_{x\in\mathbb{R}^n} \left\{K\|x-x_0\|^\alpha - P^{-1}\lambda^{-P}\|x-z\|^P\right\} \\
&\leq 2\sup_{x\in\mathbb{R}^n} \left\{K\|x-z\|^\alpha + K\|z-x_0\|^\alpha - P^{-1}\lambda^{-P}\|x-z\|^P\right\}.
\end{aligned}$$

By optimising in x and y, we obtain

$$\beta_{b_{p,\lambda}}(f)(z) \leq C\left(\lambda^{\frac{\alpha P}{P-\alpha}} + \|z-x_0\|^\alpha\right).$$

■

These bounds have been empirically validated in [13, 14] using the Weierstrass function and multifractals Riemann Series and Mandelbrot binomial measure.

At this point, we can compare the local version of the exponent estimate (47) in the one-dimensional case, $x, x_0 \in \mathbb{R}$:

$$\beta_{b_{P,\lambda}}(f)(x) \leq C\left(\lambda^{\frac{P\alpha}{P-\alpha}} + |x-x_0|^\alpha\right),$$

with Jaffard and Meyer's exponent estimate using wavelets (7) (we use a similar notation for the wavelet scale),

$$|Wf(x,\lambda)| \leq A\lambda^{\alpha+1/2}\left(1+\left|\frac{x-x_0}{\lambda}\right|^\alpha\right) = A\lambda^{1/2}\left(\lambda^\alpha + |x-x_0|^\alpha\right).$$

with $\alpha \leq n$, where n the number of vanishing moments of the wavelet. In both cases, the necessary condition is f to be α-Hölder. However, as pointed out by [13], the reciprocal is not fully obtained with linear wavelet. Indeed, the corresponding expression is as follows from (2): there exist A and $\alpha' < \alpha$ such that if

$$|Wf(x,\lambda)| \leq A\lambda^{\alpha+1/2}\left(1+\left|\frac{x-x_0}{\lambda}\right|^{\alpha'}\right) = A\lambda^{1/2}\left(\lambda^\alpha + \lambda^{\alpha-\alpha'}|x-x_0|^{\alpha'}\right),$$

then f is α-Hölder at x_0.

However, from our viewpoint, the main interest of the morphological analysis is the natural way to extend the Euclidean results to any general length space.

6 Morphological multiscale analysis on the lattice of Hölder functions on metric spaces

We have shown how the morphological gradient and its total variation can be used to estimate the fractal dimension of signal and images on Euclidean spaces. On the other hand, Hölder

exponent and fractal dimension are closely related and the variation of the morphological gradient is bounded by a function on the Hölder exponent.

In this section, we focus on the nonlinear analysis of Hölder functions on metric spaces using morphological semigroups. These functions are therefore in the sublattice of equicontinuous $\bar{\mathcal{L}}_m$, where continuity modulus will be of the form $m(h) = Kh^\alpha$. The following well known result is important to realize that Lipschitz and Hölder functions are qualitatively similar in many cases.

Lemma 13 *Let (X, d) be a metric space and $f : X \to \mathbb{R}$ a real-valued bounded Lipschitz function with constant K and $|f(x)| \leq M$. Then f is α-Hölder too.*

Proof. Let us first consider that $d(x, y) \leq 1$. Because $\alpha \in (0, 1)$, one has

$$|f(x) - f(y)| \leq Kd(x, y) = Kd(x, y)^\alpha d(x, y)^{1-\alpha} \leq Kd(x, y)^\alpha.$$

For $d(x, y) > 1$, we have

$$|f(x) - f(y)| \leq |f(x)| + |f(y)| \leq 2M \leq 2Md(x, y)^\alpha$$

■

Note also that any Lipschitz function on a bounded domain is bounded, so the lemma holds in particular for Lipschitz functions on bounded domains.

In the example of the lemma, but also in general, one has using (21)

$$m_{\text{Lipschitz}} \leq m_{\text{Hölder}} \implies \mathcal{L}_{m_{\text{Lipschitz}}} \subseteq \mathcal{L}_{m_{\text{Hölder}}}. \tag{50}$$

6.1 Dilation and erosion semigroups on the lattice of Hölder functions on length spaces

Let us now start by the following result by Gromov [19], which will provide us an initial flavour of how the constant in Lipschitz structuring functions interacts during the regularization with the α exponent.

Theorem 14 (Gromov, 1999 [19]) *Let $f : X \to \mathbb{R}$ be a real-valued function on a metric space (X, d). Let $0 < \alpha < 1$ and suppose that there exist $K > 0$ so that for each $\mu > 0$ we can find an erosion $\varepsilon_{w_{\mu^{-1}}}(f)$ with structuring function*

$$w_{\mu^{-1}}(x, y) = -\mu^{\alpha-1} d(x, y), \;\; x, y \in X$$

such that

$$\sup_X \left| f - \varepsilon_{w_{\mu^{-1}}}(f) \right| \leq K\mu^\alpha \quad \textit{and} \tag{51}$$

$$\varepsilon_{w_{\mu^{-1}}}(f) \;\; \textit{is } K\mu^{\alpha-1}\textit{-Lipschitz.} \tag{52}$$

Then f is α-Hölder continuous.

Conversely, if f is α-Hölder continuous, then for each μ there is a function $\varepsilon_{w_{\mu^{-1}}}(f)$ which satisfies (51) *and* (52)*, with K taken to be the Hölder constant of f.*

Proof. We follows [19](Theorem B.6.16). Suppose that f is given and that K and $\varepsilon_{w_{\mu^{-1}}}(f)$ exists as said in the theorem. Let $x, y \in X$ be given, the goal is to estimate $|f(x) - f(y)|$. Set $\mu = d(x, y)$. One has

$$\begin{aligned} |f(x) - f(y)| &\leq |f(x) - \varepsilon_{w_{\mu^{-1}}}(f)(x)| + |\varepsilon_{w_{\mu^{-1}}}(f)(x) - \varepsilon_{w_{\mu^{-1}}}(f)(y)| + |f(y) - \varepsilon_{w_{\mu^{-1}}}(f)(y)| \\ &\leq K\mu^{\alpha} + K\mu^{\alpha-1}d(x, y) + K\mu^{\alpha} \\ &\leq 3Kd(x, y)^{\alpha}. \end{aligned} \tag{53}$$

Thus f is Hölder continuous of exponent α with constant $3K$.

For the second half of the theorem, let $f : X \to \mathbb{R}$ be given and consider it α-Hölder. We may also aussume the its constant is ≤ 1, since we can always achieve this normalization by dividing f by a constant. Let μ be given such as

$$\varepsilon_{w_{\mu^{-1}}}(f)(x) = \inf_{y \in X} \left\{ f(y) + \mu^{\alpha-1}d(x, y) \right\}.$$

We view $f(y) + \mu^{\alpha-1}d(x, y)$ here as a function of x, with y as a parameter. As a function x it is Lipschitz of constant $\mu^{\alpha-1}$ because $d(x, y)$ is 1-Lipschitz as a function of x, just by the triangular inequality. Using Serra's theorem 5 on the fact that the class of m-continuous functions $\bar{\mathcal{L}}_m$ and considering the case $m(h) = \mu^{\alpha-1}h$, we have that $\varepsilon_{w_{\mu^{-1}}}(f)(x)$ is also $\mu^{\alpha-1}$-Lipschitz if it is finite. Let us address that point.

We can consider a localized expression for the erosion $\varepsilon_{w_{\mu^{-1}}}(f)(x)$. Namely

$$\varepsilon_{w_{\mu^{-1}}}(f)(x) = \inf_{y \in X} \left\{ f(y) + \mu^{\alpha-1}d(x, y) \ : \ d(x, y) \leq \mu \right\}. \tag{54}$$

Indeed, since $\alpha < 1$, if $d(x, y) > \mu$ then

$$f(y) + \mu^{\alpha-1}d(x, y) > f(y) + d(x, y)^{\alpha}.$$

Thus we get that $f(y) + \mu^{\alpha-1}d(x, y) > f(x)$ since we assume

$$|f(x) - f(y)| \leq Cd(x, y)^{\alpha}, \ \ C < 1.$$

That means that y cannot contribute to the infimum in $\varepsilon_{w_{\mu^{-1}}}(f)(x)$, because it gives a larger value than $y = x$ does. This proves (54). From (54) and the Hölder continuity of f it follows that $\varepsilon_{w_{\mu^{-1}}}(f)(x)$ is finite and so $\mu^{\alpha-1}$-Lipschitz.

Again from (54), given $y \in M$ with $d(x, y) \leq \mu$, we can use Hölder continuity on f to get

$$f(x) \leq f(y) + d(x, y)^{\alpha} \leq f(y) + \mu^{\alpha} \leq f(y) + \mu^{\alpha-1}d(x, y) + \mu^{\alpha}$$

taking the infimum over y we get

$$f(x) \leq \varepsilon_{w_{\mu^{-1}}}(f)(x) + \mu^{\alpha},$$

which combined with the fact that $\varepsilon_{w_{\mu^{-1}}}(f)(x) \leq f(x)$, for all $x \in X$, we obtain

$$\sup_X \left| f - \varepsilon_{w_{\mu^{-1}}}(f) \right| \leq K\mu^{\alpha}.$$

■

The power of μ in (51) and (52) may look a bit strange, but it provides the right normalization. We now introduce a more general result on α-Hölder functions which is a particular case of Serra's theory on equicontiuous dilation and erosion. However, in our case, we obtain the continuity moduli explicitely, without the need of the Hausdorff distance between structuring functions.

Theorem 15 *Let f be a real-valued function on the compact length space (X, d) with $f \in \bar{\mathcal{L}}_m$, where $m(d(x,y)) = Kd(x,y)^{\alpha}$, $0 < \alpha < 1$, $K > 0$. For each power $P > 1$ and scale $t > 0$, let us consider the multi-scale structuring function*

$$w_{P,t}(x,y) = -\frac{d(x,y)^P}{Pt^{P-1}}. \tag{55}$$

Then, the dilation $D_{P,t}(f)$ and erosion $E_{P,t}(f)$ defined respectively by (30) and (31) belong to the class $f \in \bar{\mathcal{L}}_{m'}$ of Lipschitz functions, $m'(d(x,y)) = K_{P,t}d(x,y)$, i.e.,

$$|D_{P,t}(f)(x) - D_{P,t}(f)(y)| \leq K_{P,t}d(x,y) \tag{56}$$

$$|E_{P,t}(f)(x) - E_{P,t}(f)(y)| \leq K_{P,t}d(x,y) \tag{57}$$

with constant

$$K_{P,t} = 2K^{\frac{P-1}{P-\alpha}} P^{\frac{\alpha-1}{P-\alpha}} t^{\frac{(1-P)^3}{P-\alpha}}. \tag{58}$$

In addition, one has the following bound on the variation

$$\sup_X |f - D_{P,t}(f)| \leq K^{\frac{P}{P-\alpha}} P^{\frac{\alpha}{P-\alpha}} t^{\frac{(P-1)\alpha}{P-\alpha}}, \tag{59}$$

$$\sup_X |f - E_{P,t}(f)| \leq K^{\frac{P}{P-\alpha}} P^{\frac{\alpha}{P-\alpha}} t^{\frac{(P-1)\alpha}{P-\alpha}}. \tag{60}$$

Proof. Because (X, d) is a compact metric space, we can assume that X is a bounded domain.

Let us first study the modulus of continuity of the structuring function $w_{P,t}(x,y)$. We fix $x \in X$ and consider it as a function of y. Then, one has

$$\begin{aligned} |w_{P,t}(x,y) - w_{P,t}(x,z)| &= \left| \frac{d(x,y)^P}{Pt^{P-1}} - \frac{d(x,z)^P}{Pt^{P-1}} \right| \quad \forall z, y \in X \\ &= P^{-1}t^{1-P} \left| d(x,y)^P - d(x,z)^P \right|, \quad \forall z, y \in X, \end{aligned}$$

note that $K' = P^{-1}t^{1-P} > 0$. Then, using the triangular inequality of the distance function and the fact that X is bounded, and thus the distance too by the diameter $\operatorname{diam}(X)$, one obtain

$$\begin{aligned} |w_{P,t}(x,y) - w_{P,t}(x,z)| &\leq P^{-1}t^{1-P}d(y,z)^P, \quad \forall z,y \in X, \\ &\leq P^{-1}t^{1-P}\operatorname{diam}(X)^{P-1}d(y,z), \quad \forall z,y \in X \end{aligned}$$

So, the structuring function is Lipschitz continuous: $m_{P,t}(d(x,y)) = P^{-1}t^{1-P}\operatorname{diam}(X)^{P-1}d(x,y)$.

Next, starting from the definition of the dilation metric semigroup:

$$\begin{aligned} D_{P,t}(f)(x) &= \sup_{y\in X}\{f(y) + w_{P,t}(y,x)\} \\ &= \sup_{y\in X}\left\{f(y) - P^{-1}t^{1-P}d(y,x)^P\right\}, \end{aligned}$$

we view $f(y) - w_{P,t}(x,y)$ here as a function of x, with y as a parameter. As a function x it is Lipschitz of constant $P^{-1}t^{1-P}\operatorname{diam}(X)^{P-1}$ because $w_{P,t}(x,y)$ is Lipschitz as a function of x with that constant. Using Serra's theorem 5 on the fact that the class of m-continuous functions $\bar{\mathcal{L}}_m$ is closed under the supremum, we have that $D_{P,t}(f)$ has modulus of continuity $m_{P,t}(d(x,y)) = P^{-1}t^{1-P}\operatorname{diam}(X)^{P-1}d(x,y)$ too. An alternative proof is as follows [23]. For all $x,y \in X$, one has

$$\begin{aligned} D_{P,t}(f)(x) - D_{P,t}(f)(y) &\leq \sup_{z\in X}\left\{f(z) - P^{-1}t^{1-P}d(x,z)^P\right\} - \sup_{z\in X}\left\{f(z) - P^{-1}t^{1-P}d(y,z)^P\right\} \\ &\leq \sup_{z\in X}\left\{P^{-1}t^{1-P}\left[d(x,z)^P - d(y,z)^P\right]\right\} \\ &\leq \left(P^{-1}t^{1-P}\sup_{z\in X}\left\{\left[d(x,z)^{P-1} + d(y,z)^{P-1}\right]\right\}\right)d(x,y) \\ &\leq 2\operatorname{diam}(X)^{P-1}P^{-1}t^{1-P}d(x,y). \end{aligned} \tag{61}$$

And similarly for the erosion semigroups.

But in the previous calculations, we did not consider any regularity for f. In our case, considering that f is α-Hölder, we will obtain a tight constant based on the fact that dilation operator can be localized in a ball. Indeed, since $D_{P,t}(f)(x) \geq f(x)$, we may restrict the supremum to points y such that

$$f(y) - P^{-1}t^{1-P}d(x,y)^P \geq f(x)$$

since we assume that f is α-Holder, i.e., $|f(x) - f(y)| \leq Kd(x,y)^\alpha$, one has

$$P^{-1}t^{1-P}d(x,y)^P \leq Kd(x,y)^\alpha$$

so we can restric the supremum to points satisfying

$$d(x,y)^P \leq KPt^{P-1}d(x,y)^\alpha \iff d(x,y) \leq \left(KPt^{P-1}\right)^{1/(P-\alpha)} = D. \tag{62}$$

That implies that the supremum of the dilation can be obtained in a ball of radius $D/2$ and noted $B_{D/2}$:

$$D_{P,t}(f)(x) = \sup_{y \in B_{D/2}(x)} \left\{ f(y) - P^{-1} t^{1-P} d(x,y)^P \right\}, \tag{63}$$

which, using the same procedure as for (61), we get

$$\begin{aligned} D_{P,t}(f)(x) - D_{P,t}(f)(y) &\leq 2D^{P-1} P^{-1} t^{1-P} d(x,y) \\ &\leq 2 \left(K P t^{P-1} \right)^{(P-1)/(P-\alpha)} P^{-1} t^{1-P} d(x,y) \\ &\leq K' d(x,y), \end{aligned}$$

with

$$K' = 2 \left(K P t^{P-1} \right)^{(P-1)/(P-\alpha)} P^{-1} t^{1-P} = 2 K^{\frac{P-1}{P-\alpha}} P^{\frac{\alpha-1}{P-\alpha}} t^{\frac{(1-P)^3}{P-\alpha}}$$

Similarly for the erosion semigroups.

For the bound on the difference between f and its dilation, we used the expression of the localized dilation (63), given $y \in M$ with $d(x,y) \leq D$ and the Hölder continuity on f such that

$$f(x) \leq f(y) - K d(x,y)^\alpha \leq f(y) - P^{-1} t^{1-P} d(x,y)^P \leq f(y) - P^{-1} t^{1-P} d(x,y)^P + K D^\alpha$$

taking the supremum over y we get

$$f(x) \leq D_{P,t}(f)(x) + K D^\alpha$$

which combined with the fact that $D_{P,t}(f)(x) \geq f(x)$, for all $x \in X$, we obtain

$$\begin{aligned} \sup_X |f - D_{P,t}(f)| &\leq K D^\alpha \\ &\leq K^{\frac{P}{P-\alpha}} \left(P t^{P-1} \right)^{\frac{\alpha}{P-\alpha}} \end{aligned}$$

Similarly for the erosion semigroups.

■

This result of the Lipschitz regularity of dilation and erosion on metric spaces, already considered in [23], is just the counterpart of the classical ones for equicontinuous functions on Hilbert spaces, and they are the basic ingredients for the Lasry–Lions regularization [21], which can be also studied for Riemannian manifolds [2].

Note also that in the canonical case of quadratic structuring function, i.e., $P = 2$, one gets:

$$\begin{aligned} |D_{2,t}(f)(x) - D_{2,t}(f)(y)| &\leq \left(2 K t^{-1} \right)^{\frac{1}{2-\alpha}} d(x,y), \\ \sup_X |f - D_{2,t}(f)| &\leq K^{\frac{2}{2-\alpha}} (2t)^{\frac{\alpha}{2-\alpha}}. \end{aligned}$$

6.2 Hölder exponent estimates on length spaces

The expressions of theorem 15 provides a quantitative analysis of how Hölder functions are regularized by morphological semigroups on length spaces, but they cannot easily use in practice to estimate the exponent α. Let us just show the generalization of Gondran and Kenoufi results from theorem 12 to our framework.

Theorem 16 *Let (X, d) be a compact length space . For each power $P > 1$ and scale $t > 0$, we consider the multi-scale structuring function*

$$w_{P,t}(x, y) = -\frac{d(x, y)^P}{Pt^{P-1}}. \tag{64}$$

and the corresponding metric dilation $D_{P,t}(f)$ and erosion $E_{P,t}(f)$ semigroups defined respectively by (30) *and* (31)*. The real-valued function on X, $f \in \mathcal{F}(X, \overline{\mathbb{R}})$ is α-Hölder, $0 < \alpha \leq 1$, if and only if it exists a constant C such as for $t > 0$, one has the following condition:*

$$\beta_{b_{P,t}}(f)(x) \quad \leq \quad Ct^{\frac{(P-1)\alpha}{P-\alpha}}, \tag{65}$$

with

$$C = 3K^{\frac{P}{P-\alpha}} P^{\frac{\alpha}{P-\alpha}}, \tag{66}$$

where $\beta_{P,t}(f)$ is the morphological gradient associated to the dilation and erosion semigroups, i.e.,

$$\beta_{P,t}(f)(x) = D_{P,t}(f)(x) - E_{P,t}(f)(x). \tag{67}$$

Proof. Because (X, d) is a compact metric space, we can assume that X is a bounded domain. Because X is a length space, we assume also the existence of geodesics for any pair of points.

Let us first assume that f is α-Hölder for all $x, y \in X$. As we have shown, that means that dilation and erosion can be limited to points satisfying $d(x, y) \leq \left(KPt^{P-1}\right)^{1/(P-\alpha)} = D$. Using the definition of the morphological gradient, one has

$$\begin{aligned}
\beta_{P,t}(f)(z) &= D_{P,t}(f)(z) - E_{P,t}(f)(z) \\
&= \sup_{x \in B_{D/2}} \left\{ f(x) - \frac{d(x, z)^P}{Pt^{P-1}} \right\} - \inf_{y \in B_{D/2}} \left\{ f(y) + \frac{d(z, y)^P}{Pt^{P-1}} \right\} \\
&= \sup_{x, y \in B_{D/2}} \left\{ f(x) - f(y) - \frac{d(x, z)^P}{Pt^{P-1}} - \frac{d(y, z)^P}{Pt^{P-1}} \right\}.
\end{aligned}$$

Using now Hölder continuity,

$$\begin{aligned}
\beta_{P,t}(f)(z) &\leq \sup_{x, y \in \mathbb{R}^n} \left\{ Kd(x, y)^\alpha + P^{-1}t^{1-P} \left(d(x, z)^P + d(y, z)^P \right) \right\} \\
&\leq KD^\alpha + 2P^{-1}t^{1-P}D^P.
\end{aligned}$$

Using again the fact that $d(x,y) \leq \left(KPt^{P-1}\right)^{1/(P-\alpha)} = D$, one has

$$\begin{aligned} KD^{\alpha} + 2P^{-1}t^{1-P}D^{P} &= K\,(KP)^{\frac{\alpha}{P-\alpha}}\,t^{\frac{(P-1)\alpha}{P-\alpha}} + 2P^{-1}\,(KP)^{\frac{P}{P-\alpha}}\,t^{1-P}t^{\frac{(P-1)P}{P-\alpha}} \\ &= K^{\frac{P}{P-\alpha}}P^{\frac{\alpha}{P-\alpha}}t^{\frac{(P-1)\alpha}{P-\alpha}} + 2K^{\frac{P}{P-\alpha}}P^{\frac{\alpha}{P-\alpha}}t^{\frac{(P-1)\alpha}{P-\alpha}} \\ &= \left(3K^{\frac{P}{P-\alpha}}P^{\frac{\alpha}{P-\alpha}}\right)t^{\frac{(P-1)\alpha}{P-\alpha}}. \end{aligned}$$

Conversely, let us assume first that f satisfies $\beta_{P,t}(f)(x) \leq Ct^{\frac{(P-1)\alpha}{P-\alpha}}$. We consider $x, y \in X$ with $f(x) \geq f(y)$.

Using the convergence, for any function f and $\forall x \in X$, $D_{P,t}f(x)$ and $E_{P,t}f(x)$ converge monotonically to $f(x)$ as $t \to 0$. Similar to the Euclidean case, we can use the reconstruction formula (16) of f:

$$f(x) = \inf_{\substack{t \in \mathbb{R}_+ \\ z \in \mathbb{R}^n}} \left\{D_{P,t}(f)(z) + P^{-1}t^{1-P}d(x,z)^{P}\right\},$$

and for $f(y)$ the simplified dual reconstruction (18):

$$f(y) = \sup_{\lambda \in \mathbb{R}_+} \left\{E_{P,t}(f)(y)\right\}.$$

Thus, one has

$$\begin{aligned} f(x) - f(y) &\leq \inf_{t \in \mathbb{R}_+} \left\{D_{P,t}(f)(y) + P^{-1}t^{1-P}d(x,z)^{P} - E_{P,t}(f)(y)\right\} \\ &\leq \inf_{t \in \mathbb{R}_+} \left\{Ct^{\frac{(P-1)\alpha}{P-\alpha}} + P^{-1}t^{1-P}d(x,z)^{P}\right\}. \end{aligned} \tag{68}$$

So we need to optimize at scale t on $Ct^{\frac{(P-1)\alpha}{P-\alpha}} + P^{-1}t^{1-P}d(x,y)^{P}$.

Now, by considering that there exists an α such that $t^{\frac{(P-1)\alpha}{P-\alpha}} = d(x,y)^{\alpha}$ and thus $d(x,y) = t^{\frac{(P-1)}{P-\alpha}}$, one has

$$\begin{aligned} Ct^{\frac{(P-1)\alpha}{P-\alpha}} + P^{-1}t^{1-P}d(x,y)^{P} &= Cd(x,y)^{\alpha} + P^{-1}t^{1-P}t^{\frac{(P-1)P}{P-\alpha}} \\ &= Cd(x,y)^{\alpha} + P^{-1}d(x,y)^{\alpha} \end{aligned}$$

and therefore

$$f(x) - f(y) \leq (C + P^{-1})d(x,y)^{\alpha}.$$

By considering the case $f(y) \geq f(x)$ and combining both, we get finaly

$$|f(x) - f(y)| \leq (C + P^{-1})d(x,y)^{\alpha}.$$

■

From a practical viewpoint, this is an operational result, which can be used in a similar way as the fractal dimension is estimated from the formula $\dim(\mathrm{Gr}(f)) = (n+1) - \lim_{\epsilon\to 0} \log MTV_{b_\epsilon}(f)/\log\epsilon$. Indeed, given a α-Hölder function, and by fixing $P > 0$, the expected value of the morphological gradient is:

$$\mathbb{E}\left[\beta_{P,t}(f)\right] \quad \leq \quad \mathbb{E}\left[Ct^{\frac{(P-1)\alpha}{P-\alpha}}\right].$$

On the other hand, using the corresponding morphological total variation (12): $MTV_{P,t}(f) = \int_X \beta_{P,t}(f)(x)d\mu(x)$, such that $\mathbb{E}\left[\beta_{P,t}(f)\right] = \mu(X)^{-1}MTV_{P,t}(f)$, with $\mu(X) = \int_X d\mu(x)$. Thus one has near the origin ($t \to 0$):

$$\log MTV_{P,t}(f) = \log\left(C\mu(X)\right) + \left[\frac{(P-1)\alpha}{P-\alpha}\right]\log t, \tag{69}$$

and therefore, the slope s from the linear regression near the origin of the log-log curve $\log t \mapsto \log MTV_{P,t}(f) = a + s\log t$, provides the value of the Hölder exponent:

$$\alpha = \frac{Ps}{(P-1)+s}. \tag{70}$$

6.3 Experimental validation

In order to validate the practical interest of the theory, we use a similar experimental setup to the one considered above for the fractal dimension.

We deal with the case of fractional Brownian surfaces $B_H(x,y)$, with Hurst parameter $0 < H < 1$, such that the fractal dimension is $\dim_{\mathrm{M}} = 3 - H$: low H implies high fractal dimension (more rough surface). We remind that a $B_H(x,y)$ is a Hölder continuous function and the H provides an upper (tight) bound of the pointwise α-Hölder exponent. It is typically considered that the fractional Brownian surfaces are an appropriate random model to study Hölder continuity and that for a given fractional Brownian surface, in average the Hölder exponent can be prescribed via its Hurst parameter, i.e., $\alpha = H$. For each experience, we have simulated 50 realizations of $B_H(x,y)$ with a given value of Hurst exponent H and we have extracted a fractal image field f of 500×500 pixels from each realisation. We have considered five exponents: $H = 0.1$, $H = 0.3$, $H = 0.5$, $H = 0.7$ and $H = 0.9$, see for instance the examples provided in Fig 2.

Let us describe how the approach is implemented. The key element is the morphological metric gradient (67) $\beta_{P,t}(f)(x)$, which requires the computation of the pair of multiscale dilation $D_{P,t}(f)(x)$ and erosion $E_{P,t}(f)(x)$. For them, the main ingredient is the multiscale structuring function:

$$w_{P,t}(x,y) = -\frac{d(x,y)^P}{Pt^{P-1}}, \tag{71}$$

which depends on the shape parameter P and scaling t. In practice, we need a discretization of $w_{P,t}(x,y)$. For the current case, $x, y \in X \subset \mathbb{Z}^2$, where X is the 500×500 domain of the 2D discrete image of the fractional Brownian field and $d(x,y)$ is just a normalized Euclidean distance between x and y coordinates. In order to have a satisfactory discretization of the shape function, we have considered a local neighbourhood for $w_{P,t}(x,y)$ of $L \times L$ pixels, typically $L = 21$ or $L = 15$. Outside this local window, one considers that $w_{P,t}(x,y) = -\infty$. The choice of an appropriate scaling t depends on both the distance and the dynamic range of the image $\mathrm{rg}f$, i.e., $\mathrm{rg}f = \max f - \min f$. Typically, in our images, $\mathrm{rg}f \approx 3$. We propose the following normalization of the distance:

$$d(x,y) = \frac{\|x-y\|_2}{L^2}\mathrm{rg}f$$

Figure 5 illustrates some examples of structuring functions $w_{P,t}(x,y)$ seen as an image, with $L = 21$ and $\mathrm{rg}f = 3$, for three values of P (1.5, 2 and 4) and three values of t (0.01, 0.1 and 1). We note that when P increases, the shape becomes flatter. By checking the scale of the intensity, we note that increasing t implies values closer to 0, therefore a similar penalization into the whole neighbourhood, which for a large window yields to an imprecise structuring function to capture for fast local variations.

Because we need to compute a series of multiscale dilations and erosions, we propose to use the semigroup property and compute them using an iterative algorithm starting from the initial scale t_0. The idea for the dilation at the n-th scale is as follows:

$$\begin{aligned} D_{P;\,t_0} f(x) &= \sup_{y \in X} \{f(y) + w_{P,t_0}(x,y)\} \\ &= \sup_{y \in X} \left\{ f(y) - \frac{d(x,y)^P}{Pt^{P-1}} \right\}, \\ D_{P;\,t=nt_0} f(x) &= D_{P;\,t_0}\left(D_{P;\,(n-1)t_0} f\right)(x) \\ &= \sup_{y \in X} \left\{ \left(D_{P;\,(n-1)t_0} f\right)(y) - \frac{d(x,y)^P}{Pt^{P-1}} \right\}, \quad n = 2, 3, \cdots N. \end{aligned}$$

So finally, the important choice is the smallest scale $t = t_0$ and the number N of considered scales. In the Figure 6 gives some examples of the morphological metric gradient (67) $\beta_{P,t=nt_0}(f)(x)$ from an image f, with the parameters $L = 15$, $P = 2$ and $t_0 = 0.1$. That illustrates well how the multiple scales of variation of the image are locally captured.

We note that this implementation using the semigroup is valid for any length space. In the case of a metric space, one should implement the specific metric dilation and erosion with the structuring function at scale t. From a practical viewpoint, the main difficulty would be the need of a local window for the discretization of the structuring function which should of larger size in order to capture the evolution of $w_{P,t}$ with respect to t.

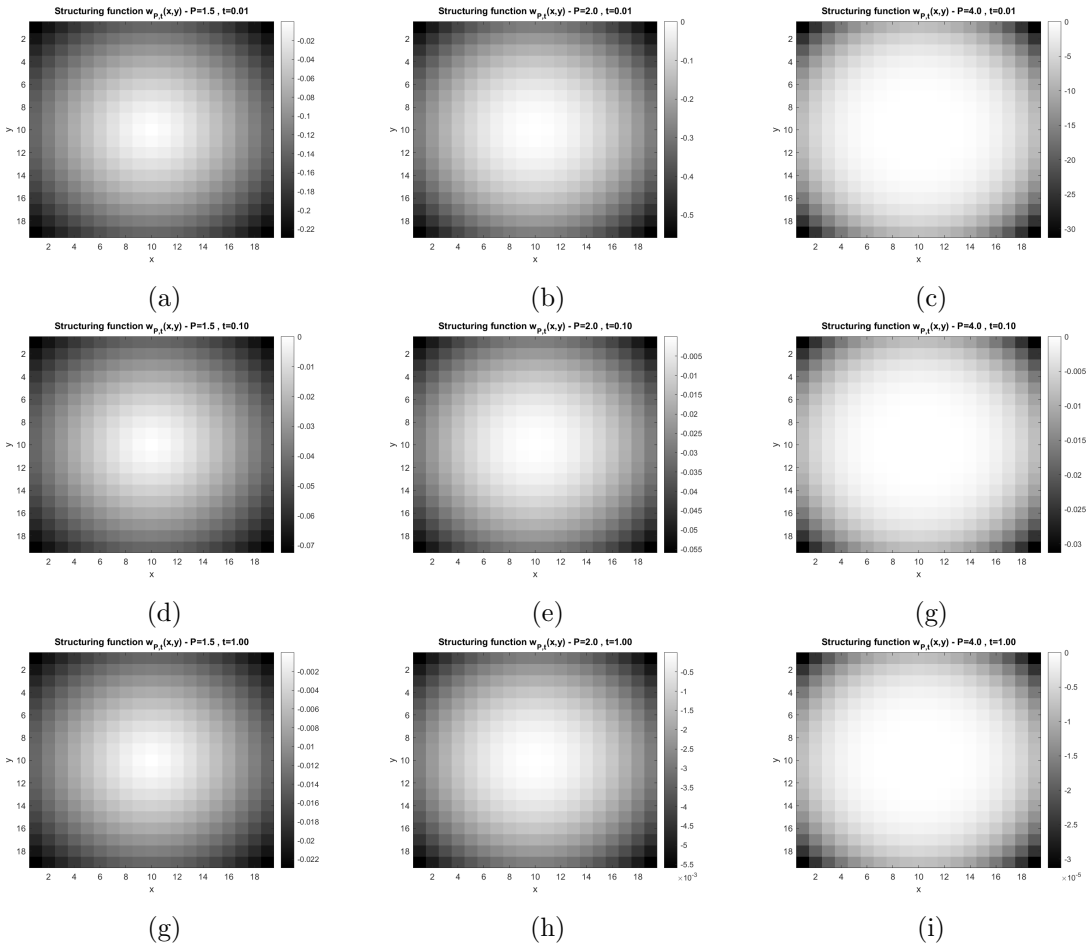

Figure 5: Examples of structuring functions $w_{P,t}(x, y)$ in a window of 21×21 pixels and rg$f = 3$: (a) $P = 1.5$, $t = 0.01$ (scale 0 to -0.22), (b) $P = 2$, $t = 0.01$ (scale 0 to -0.5), (c) $P = 4$, $t = 0.01$ (scale 0 to -30), (d) $P = 1.5$, $t = 0.1$ (scale 0 to -0.07), (e) $P = 2$, $t = 0.1$ (scale 0 to -0.05), (f) $P = 4$, $t = 0.1$ (scale 0 to -0.03), (g) $P = 1.5$, $t = 1$ (scale 0 to -0.02), (h) $P = 2$, $t = 1$ (scale 0 to -0.05), (i) $P = 4$, $t = 1$ (scale 0 to -0.00003).

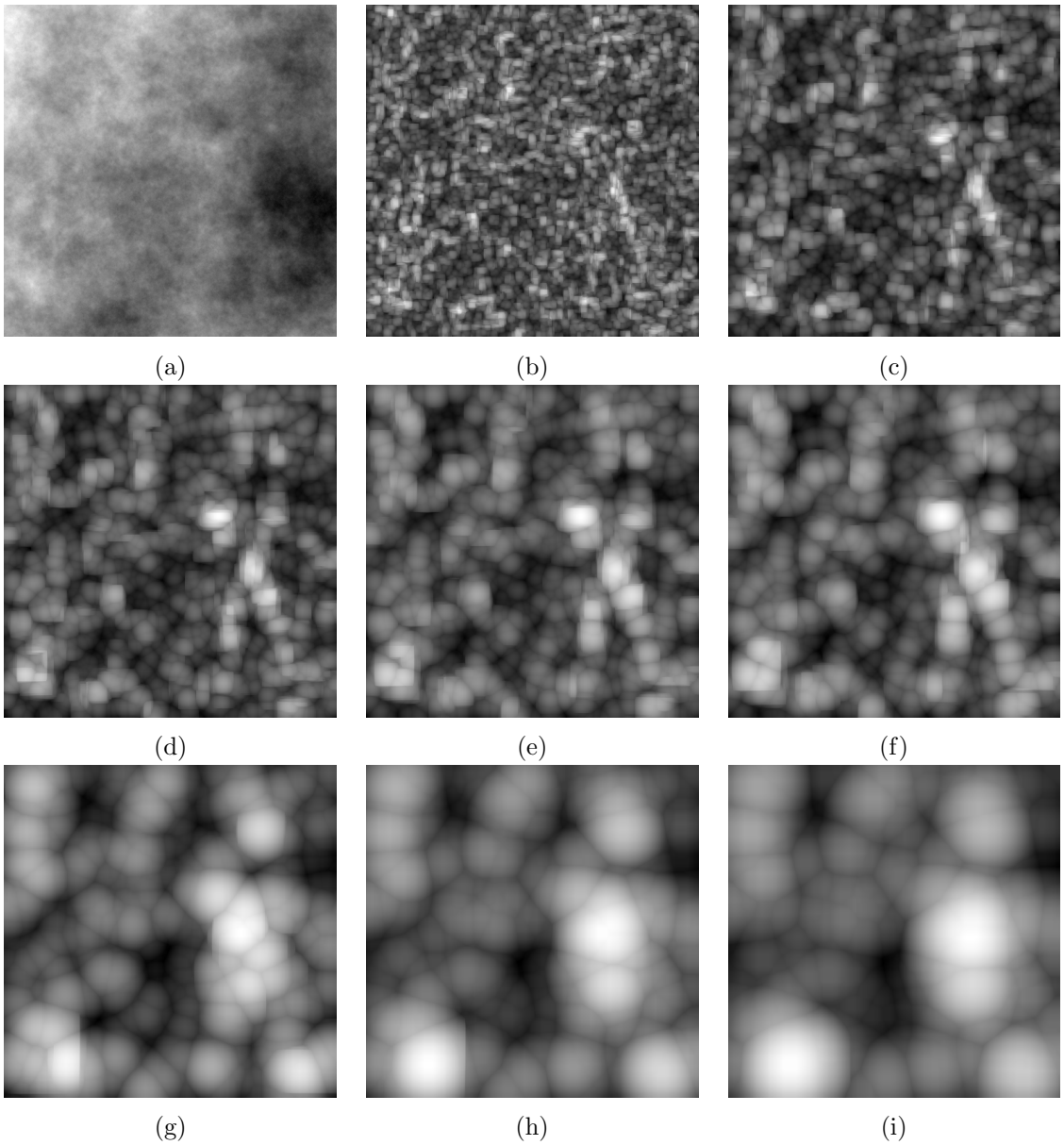

Figure 6: Examples of the morphological metric gradient $\beta_{P,t=nt_0}(f)(x)$, with parameters for structuring function ($L = 15$, $P = 2$ and $t_0 = 0.1$): (a) original image f ($H = 0.7$), (b) $t = t_0$, (c) $t = 2t_0$, (d) $t = 3t_0$, (e) $t = 4t_0$, (f) $t = 5t_0$, (g) $t = 10t_0$, (ah) $t = 15t_0$, (i) $t = 20t_0$.

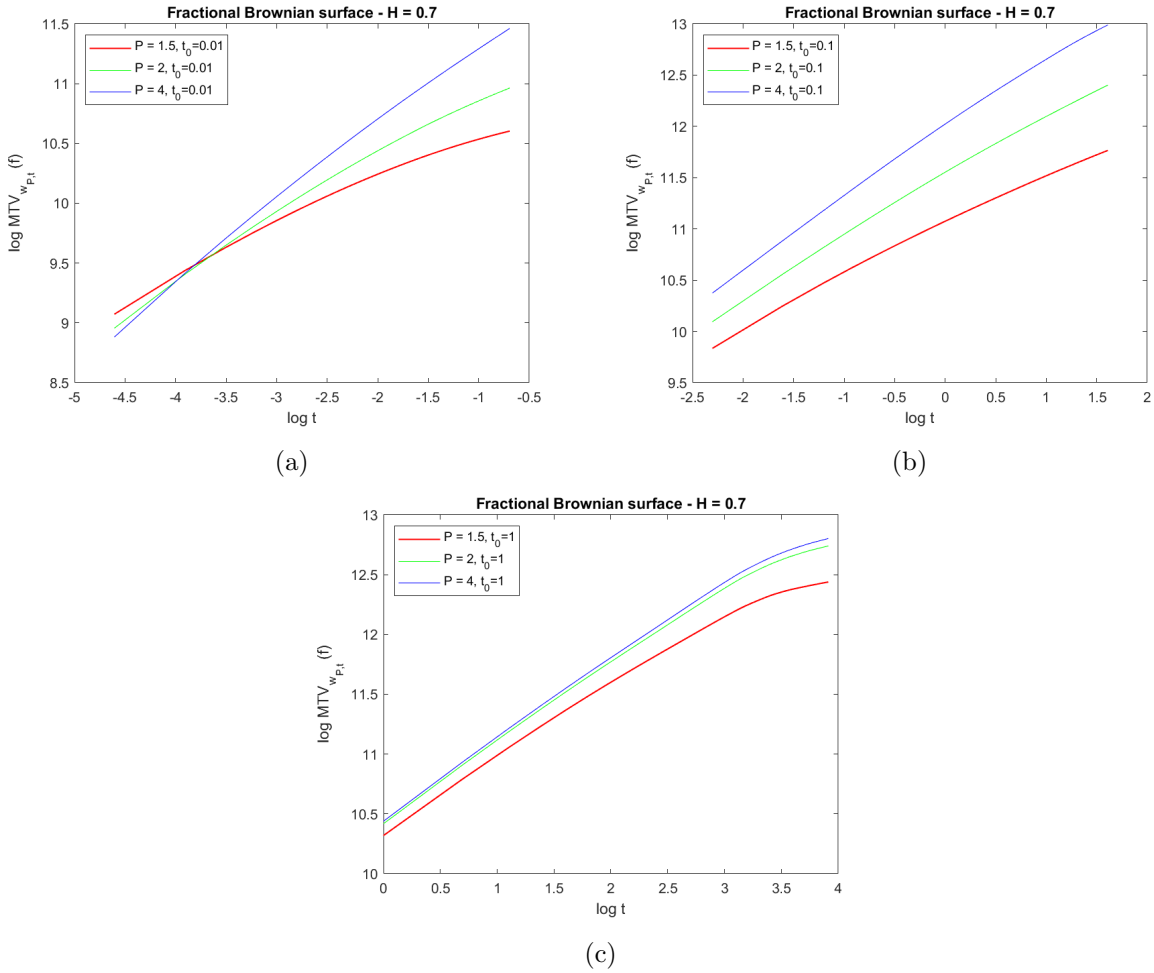

Figure 7: Graphs in $\log - \log$ scale of $(t, MTV_{P,t}(f))$ from the same fractional Brownian image field of $H = 0.7$ using three values of P (1.5, 2 and 4) for the multiscale structuring functions with window of size $L = 15$: (a) $t_0 = 0.01$, (b) $t_0 = 0.1$ and (c) $t_0 = 1$. The number of scales is always $N = 50$.

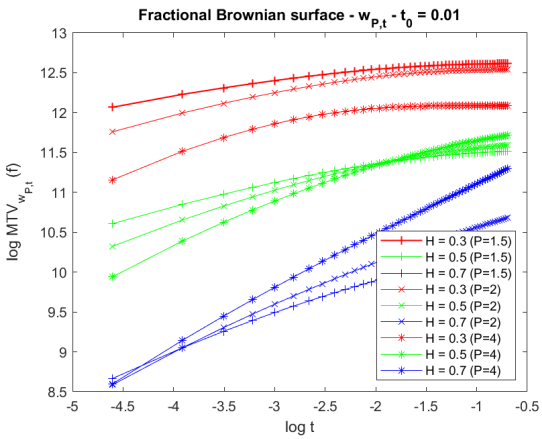

(a)

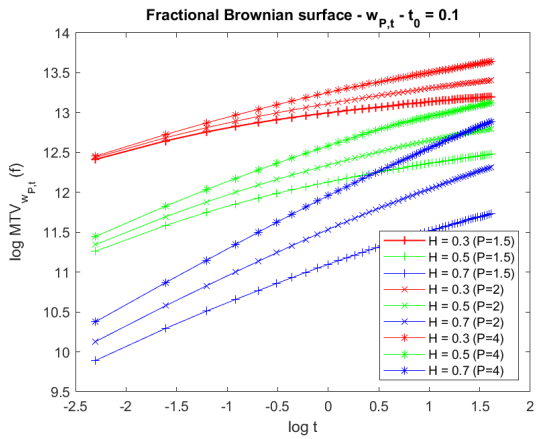

(b)

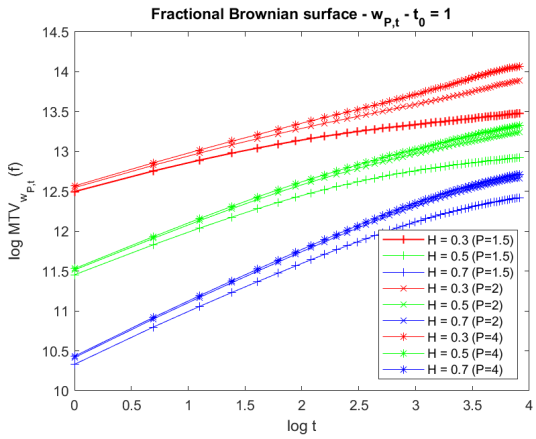

(c)

Figure 8: Graphs in $\log - \log$ scale of $(t, MTV_{P,t}(f))$ from three different fractional Brownian image fields of $H = 0.3$, 0.5 and 0.7 using three values of P (1.5, 2 and 4) for the multiscale structuring functions with window of size $L = 15$: (a) $t_0 = 0.01$, (b) $t_0 = 0.1$ and (c) $t_0 = 1$. The number of scales is always $N = 50$.

	$w_{P,t}$, $t_0 = 0.01$ (15×15 neighbourhood)					
True	$P = 1.5$		$P = 2$		$P = 4$	
H	Mean ± StdDev	Error (%)	Mean ± StdDev	Error (%)	Mean ± StdDev	Error (%)
0.1	0.15 ± 0.003	53	0.14 ± 0.004	39	0.14 ± 0.004	39
0.3	0.29 ± 0.007	1.08	0.29 ± 0.01	4.2	0.21 ± 0.04	30
0.5	0.45 ± 0.02	9.6	0.46 ± 0.03	7.0	0.49 ± 0.05	0.5
0.7	0.62 ± 0.02	11.4	0.64 ± 0.02	7.7	0.69 ± 0.03	1.5
0.9	0.79 ± 0.02	12	0.81 ± 0.04	10.2	0.81 ± 0.05	9.9

Table 2: Hölder exponent estimation α^* from fractional Brownian image samples using morphological multiscale operators, with structuring function $w_{P,t}(x, y)$ with $t_0 = 0.01$ in a window of 15×15 pixels.

	$w_{P,t}$, $t_0 = 0.1$ (15×15 neighbourhood)					
True	$P = 1.5$		$P = 2$		$P = 4$	
H	Mean ± StdDev	Error (%)	Mean ± StdDev	Error (%)	Mean ± StdDev	Error (%)
0.1	0.21 ± 0.008	114	0.22 ± 0.007	116	0.22 ± 0.008	124
0.3	0.38 ± 0.02	25.6	0.36 ± 0.02	21.3	0.35 ± 0.03	15.6
0.5	0.53 ± 0.02	5.8	0.51 ± 0.02	2.5	0.48 ± 0.03	3.3
0.7	0.69 ± 0.05	1.9	0.67 ± 0.05	7.7	0.62 ± 0.05	10.6
0.9	0.83 ± 0.03	7.6	0.81 ± 0.04	9.3	0.77 ± 0.05	14

Table 3: Hölder exponent α^* estimation from fractional Brownian image samples using morphological multiscale operators, with structuring function $w_{P,t}(x, y)$ with $t_0 = 0.1$ in a window of 15×15 pixels.

Coming back to our experiences, one can now compute the morphological total variation $MTV_{P,t}(f)$ from $\beta_{P,t}(f)(x)$. Figure 7 provides the graphs of $(\log t, \log MTV_{P,t}(f))$ for the image of Figure 6. As expected according to model underlying (69), in the case of a Hölder function we get straight lines in the $\log - - \log$ scale and the corresponding fitted slope s can be used to estimate the Hölder exponent α using (70). We compared in the plots how the slope changes with respect to P for the same theoretical α, i.e., $s = ((P-1)\alpha)/(P-\alpha)$, and in each plot we used a different initial scale: $t_0 = 0.01$, $t_0 = 0.1$ and $t_0 = 1$, with the same number of scales $t = nt_0$, $n = 1, \cdots 50$. As expected too, increasing t_0 reduces the influence of P. We observe that when t_0 is small, by taking a large enough number of scales, the precision on α expected from different values of P and associated to different slopes, is higher than when t_0 is large. In the Figure 8, the same curves are now compared from three different fractional Brownian image fields of $H = 0.3$, 0.5 and 0.7. We note that for all choices of P and t_0, the intercept of the curve is a good indicator to separate the different exponents, but unfortunately that cannot be used in practice to estimate α since the constant K is unknown.

	$w_{P,t}$, $t_0 = 1$ (15×15 neighbourhood)					
True	$P = 1.5$		$P = 2$		$P = 4$	
H	Mean ± StdDev	Error (%)	Mean ± StdDev	Error (%)	Mean ± StdDev	Error (%)
0.1	0.27 ± 0.006	172	0.26 ± 0.01	163	0.23 ± 0.02	135
0.3	0.46 ± 0.02	52	0.44 ± 0.03	47.4	0.38 ± 0.03	26.5
0.5	0.63 ± 0.03	27	0.61 ± 0.04	22.1	0.53 ± 0.05	7
0.7	0.74 ± 0.03	6.3	0.71 ± 0.05	1.4	0.63 ± 0.06	9.9
0.9	0.86 ± 0.04	3.7	0.83 ± 0.05	7.6	0.77 ± 0.06	14.4

Table 4: Hölder exponent α^* estimation from fractional Brownian image samples using morphological multiscale operators, with structuring function $w_{P,t}(x, y)$ with $t_0 = 1$ in a window of 15×15 pixels.

Qualitatively, for a given P and t_0, a higher slope implies a higher α.

Let us conclude with the quantitative analysis. Tables 2 (for $t_0 = 0.01$), 3 (for $t_0 = 0.1$) and 4 (for $t_0 = 1$) provide the summary of the experiments with this set of parameters discussed above. The estimated Hölder exponent α^α, sample mean and standard deviation for 50 random realizations, and the percent estimation error $|H - \alpha^\alpha|/ H$. The three shapes of structuring functions with respect to P are compared. Even if the percent estimation error can look very large, note that we are just estimation a value in the interval 0 to 1. With a low t_0, we note that for most of the cases, the absolute error is typically < 0.1.

7 Conclusions and perspectives

The use of morphological operators for the estimation of the Minkoswki dimension from fractal functions or the exponent from Hölder functions is a classic topic. We have revisited this problem as well as some recent contributions from the field of max-plus mathematics, which are strongly related to mathematical morphology. This classical setting is formulated for functions on $\mathbb{R}^n$. Mathematical morphology operators can be extended to functions on length spaces, including the corresponding Hamilton–Jacobi partial differential equations and their solutions as morphological semigroups. We have shown that Hamilton–Jacobi semigroups on length spaces are the main ingredients to characterize Hölder functions on that rather general spaces. Indeed, Euclidean and Riemannian manifolds belong to this class, as well as other discrete geodesic spaces such as networks. The theory of this paper provides an alternative approach to wavelets as tool to characterize Hölder functions. From our viewpoint, morphological semigroups are more naturally extended to non-Euclidean spaces than wavelets. In addition, in the case of high dimensional vector spaces, morphological semigroups are also efficiently computed, i.e., the basic ingredient is just the distance between points.

Two main applications of this theory can be considered in the field of image and data analysis. The first one is the morphological sampling of real-valued functions on high dimensional spaces. The second one is the formulation of ad-hoc architectures of neural networks which would be adapted to predict fractal dimension and similar underlaying regularity parameters of functions such as textures, sounds or other physical signals.

Finally, it exists nowadays fractal models for surfaces and field over Riemannian manifolds, in particular fractional Brownian models [18, 48, 35]. Our morphological framework on metric spaces can be applied to the Riemannian manifold case.

References

[1] J. Angulo, S. Velasco-Forero. Riemannian Mathematical Morphology. *Pattern Recognition Letters*, 47:93–101, 2014.

[2] J. Angulo. Lipschitz Regularization of Images supported on Surfaces using Riemannian Morphological Operators. hal-01108130v2, 2014.

[3] J. Angulo. Morphological PDE and dilation/erosion semigroups on length spaces. In *Proc. of ISMM'15 (12th International Symposium on Mathematical Morphology)*, LNCS 9082, Springer, pp. 509–521, 2015.

[4] G. Birkhoff. *Lattice Theory.* Vol. 25, American Mathematical Society, 3rd Ed., Providence, 1984.

[5] G. Bouligand. Ensembles impropres et nombre dimensionnel. Bull. Sci. Math., II-52, II-53, 1928, 1929.

[6] Z Botev. Fractional Brownian motion generator. https://www.mathworks.com/matlab central/fileexchange/38935-fractional-brownian-motion-generator, *MATLAB Central File Exchange.* Retrieved July, 2020.

[7] Z. Botev. Fractional Brownian field or surface generator. https://www.mathworks.com/matlabcentral/fileexchange/38945-fractional-brownian-field-or-surface-generator, *MATLAB Central File Exchange.* Retrieved July 2020.

[8] G. Choquet. *Topology.* Academic Press, London, 1966.

[9] K. Daoudi, J. Lévy Véhel, Y. Meyer. Construction of Continuous Functions with Prescribed Local Regularity. Constructive Approximation, 14:349–385, 1998.

[10] B. Dubuc, J.F. Quiniou, C. Roques-Carmes, C. Tricot, S.W. Zucker. Evaluating the fractal dimension of profiles. *Physical Review A,* 39:1500–1512, 1989.

[11] M. Gondran. Analyse minplus. *C.R. Acad. Sci. Paris,* 323: 371–375, 1996.

[12] M. Gondran. Convergences de fonctions à valeurs dans $\mathbb{R}^k$ et analyse minplus complexe. *C.R. Acad. Sci. Paris,* 329: 783–788, 1999.

[13] M. Gondran, A. Kenoufi. Numerical calculations of Hölder exponents for the Weierstrass functions with $(\min, +)$-wavelets. *Trends in Applied and Computational Mathematics,* 15(3):261–273, 2014.

[14] M. Gondran, A. Kenoufi, T. Lehner. Multi-fractal Analysis for Riemann Serie and Mandelbrot Binomial Measure with $(\min, +)$-wavelets. *Trends in Applied and Computational Mathematics,* 17(2):247–263, 2016.

[15] F. Hausdorff. Dimension und äußeres Maß . Mathematische Annalen, 79(1–2): 157–179, 1919.

[16] H.J.A.M. Heijmans. *Morphological image operators.* Academic Press, Boston, 1994.

[17] S. Jaffard, Y. Meyer. *Wavelet Methods for Pointwise Regularity and Local Oscillations of Functions.* Vol. 123, American Mathematical Society, Providence, 1996.

[18] Z.A. Gelbaum. Fractional Brownian fields over manifolds *Trans. Amer. Math. Soc.,* 366(9):4781–4814, 2014.

[19] M. Gromov. *Metric Structures for Riemannian and Non-Riemannian Spaces.* Birkhäuser, Boston, 2001.

[20] D.P. Kroese, Z.I. Botev. Spatial Process Simulation. In *Stochastic Geometry, Spatial Statistics and Random Fields,* pp. 369–404, Springer, 2015.

[21] J.M. Lasry, P.-L. Lions. A remark on regularization in Hilbert spaces. *Israel Journal of Mathematics,* 55: 257–266, 1986.

[22] R. Lopes, N. Betrouni. Fractal and multifractal analysis: A review. *Medical Image Analysis,* 13(4): 634–649, 2009.

[23] J. Lott, C. Villani. Hamilton–Jacobi semigroup on length spaces and applications. *J. Math. Pures Appl.*, 88(3):219–229, 2007.

[24] B. Mandelbrot, J.W. van Ness. Fractional Brownian motions, fractional noises and applications. *SIAM Review,* 10 (4): 422–437, 1968.

[25] B.B. Mandelbrot. *Fractal and Chaos.* Springer, 2004.

[26] S. Mallat, S. Zhong. Characterization of signals from multiscale edges. IEEE Trans. Patt. Anal. Mach. Intell., 14(7):710–732, 1992.

[27] S. Mallat. *A Wavelet Tour of Signal Processing.* 3rd Edition, Academic Press, 2008.

[28] P. Maragos, F.-K. Sun. Measuring the fractal dimension of signals: morphological covers and iterative optimization. IEEE Trans. Signal Processing, 41(1):108–121, 1993.

[29] P. Maragos. Fractal signal analysis using mathematical morphology. In (P. Hawkes and B. Kazan, Eds.) Advances in Electronics and Electron Physics, Vol. 88: 199–246, Academic Press, 1993.

[30] P. Maragos. Slope Transforms: Theory and Application to Nonlinear Signal Processing. *IEEE Trans. on Signal Processing,* 43(4): 864–877, 1995.

[31] P. Maragos, A. Potamianos. Fractal dimensions of speech sounds: computation and application to automatic speech recognition. *J Acoust Soc Am.,* 105(3):1925–1932, 1999.

[32] M. Minoux, M. Gondran. *Graphs, Dioids and Semirings.* Springer, 2008.

[33] H. Minkowski. Über die Begriffe Länge, Oberfläche, und Volumen. Jahresbericht der Deutschen Mathematiker Vereinigung, 9: 115–121, 1901.

[34] P. Moreau, Ch. Ronse. Generation of Shading-Off in Images by Extrapolation of Lipschitz Functions. *Graphical Models and Image Processing,* 58(4): 314–333, 1996.

[35] H. Rabiei, O. Coulon, J. Lefèvre, F.J.P. Richard. Surface Regularity via the Estimation of Fractional Brownian Motion Index. *IEEE Transactions on Image Processing,* 30:1453–1460, 2021.

[36] J.-P. Rigaut. Automated image segmentation by mathematical morphology and fractal geometry. Journal of Microscopy, 150(Pt. 1): 21–30, 1988.

[37] J.-F. Rivest, P. Soille, and S. Beucher. Morphological gradients. Journal of Electronic Imaging, 2(4): 326–336, 1993.

[38] M.R. Schroeder *Fractals, Chaos, Power Laws: Minutes from an Infinite Paradise.* W.H. Freeman & Company, New York, 1991

[39] J. Serra. *Image Analysis and Mathematical Morphology.* Academic Press, London, 1982.

[40] J. Serra. *Image Analysis and Mathematical Morphology. Vol II: Theoretical Advances,* Academic Press, London, 1988.

[41] J. Serra. Equicontinuous functions: A model for mathematical morphology. In *Image Algebra and Morphological Image processing III, SPIE Vol. 1769,* 252–263, 1992.

[42] J. Serra. A Sampling Approach Based on Equicontinuity. In *Serra J., Soille P. (eds) Mathematical Morphology and Its Applications to Image Processing. Computational Imaging and Vision, Vol 2,* 117–124, Kluwer, 1994.

[43] J. Serra. Equicontinuous random functions. *Journal of Electronic Imaging,* 6(1): 7 – 15, 1997.

[44] W. Shen. Hausdorff dimension of the graphs of the classical Weierstrass functions. *Mathematische Zeitschrift,* 289(1–2): 223–266, 2018.

[45] P. Soille, J.-F. Rivest. On the Validity of Fractal Dimension Measurements in Image Analysis Journal of Visual Communication and Image Representation, 7(3): 217–229, 1996.

[46] C. Tricot, J.F. Quiniou, D. Wehbi, C. Roques-Carmes, B. Dubuc. Evaluation de la dimension fractale d'un graphe. *Rev. Phys. Appl. (Paris),* 23(2):111–124, 1988

[47] C. Tricot. *Courbes et dimension fractale.* Springer, 1993.

[48] N. Venet. On the existence of fractional Brownian fields indexed by manifolds with closed geodesics. *arXiv,* 1612.05984, 2016.